SONIC LIMIT SINGULARITIES IN THE HODOGRAPH METHOD

by

Steven H. Schot

Thesis submitted to the Faculty of the Graduate School
of the University of Maryland in partial fulfillment
of the requirements for the degree of
Doctor of Philosophy
1958

APPROVAL SHEET

Title of Thesis: Sonic Limit Singularities in the Hodograph Method

Name of Candidate: Steven H. Schot
Doctor of Philosophy, 1958

Thesis and Abstract Approved: Geoffrey S. S. Ludford

Geoffrey S. S. Ludford
Associate Professor
Department of Mathematics and
Institute for Fluid Dynamics and Applied Mathematics

Date Approved: May 2, 1958

ABSTRACT

Title of Thesis: Sonic Limit Singularities in the Hodograph Method

Steven Henry Schot, Doctor of Philosophy, 1958

Thesis directed by: Sup.: Geoffrey S. S. Ludford, Associate Professor
Department of Mathematics and Institute for Fluid Dynamics and Applied Mathematics.

In the hodograph transformation, introduced to linearize the equations governing the two-dimensional inviscid potential flow of a compressible fluid, there may appear so-called limit-points and limit-lines at which the Jacobian $J = \partial(x,y)/\partial(q,\theta)$ of the transformation vanishes. This thesis investigates these singularities when they occur at points or segments of arc of the sonic line (Mach number unity).

Assuming the streamfunction to be regular in the hodograph variables, it is shown that sonic limit points cannot be isolated but must lie on a supersonic limit line or form a sonic limit line [cf. H. Geiringer, Math. Zeitschr., 63, (1956), 514-524]. Using this dichotomy a classification of sonic limit points is set up and certain geometrical properties of the mapping in the neighborhood of the singularity are discussed. In particular the general sonic limit line is shown to be an equipotential and an isovel; an envelope of both families of characteristics; and the locus of cusps of the streamlines and the isoclines. Flows containing sonic limit lines may be constructed by forming suitable linear combinations of the Chaplygin product solutions for any value of the separation constant $n \geq 0$. For n less than a certain value n_0 and greater than zero ($n = 0$ corresponds to the well-known radial flow), these flows represent a compressible

analogue of the incompressible corner flows and may be envisaged as taking place on a quadruply-sheeted surface. The sheets are joined at a supersonic limit line and at the sonic limit line which has the shape of a hypocycloid ($n > 1$), cycloid ($n = 1$), or epicycloid ($n < 1$). To exemplify the general behavior, the flows are constructed explicitly for $n = \frac{1}{2}$, 1, and 2. The shape of the sonic limit line is also discussed when solutions corresponding to different n are superposed, and it is shown how then the supersonic limit line can be eliminated so that an isolated sonic limit line is obtained. A flow containing such an isolated sonic limit line is presented. An appendix derives the asymptotic solution for large values of n which corresponds to the sonic limit solution.

The above results have been published in part in Math. Zeitschr., 67, (1957), 229-237. Other portions of this thesis will appear in two papers in Archive Rational Mech. and Anal., 2, (1958).

ACKNOWLEDGMENTS

I am sincerely grateful to Professor Geoffrey S. S. Ludford for his unending patience and encouragement, and his inspiring guidance in the preparation of this thesis.

I also extend my thanks to Mrs. J. L. Vanderslice for her painstaking typing of the manuscript.

This research was supported by the Office of Ordnance Research, U. S. Army, under Contract No. DA-36-034-ORD-1486 with the University of Maryland.

TABLE OF CONTENTS

I. Introduction. One method of obtaining exact solutions of the non-linear partial differential equations which govern the plane steady irrotational non-viscous flow of a compressible gas is the so-called hodograph method. This method, first introduced by Chaplygin [1], consists in making a transformation from the physical plane of flow variables x,y to the hodograph plane of velocity components u,v (or equivalently q,θ) so as to linearize the equations of motion. The problem has then been reduced to finding a solution of the linear equations in the hodograph plane and applying the inverse mapping to determine the corresponding flow in the physical plane.

One of the difficulties in the method is that the inverse mapping may break down, i.e. there may be lines in the physical plane along which the Jacobian of the hodograph transformation vanishes, and in the neighborhood of such lines a multiply-covered region in the physical plane corresponds to a simply-covered region in the hodograph plane. Such singular curves in the physical plane are called limit lines and their hodograph images critical curves* [21]. It is precisely this breakdown of the mapping which is one of the salient features of nonlinearity in the underlying equations.

It is well-known that limit lines cannot occur in the subsonic region (cf. Sec. II).

---

* Sometimes we will use the term limit line loosely to refer to the breakdown curve in the hodograph also, in the same sense that the term "streamline" is used to denote the curve in the physical plane as well as its hodograph image.

In the supersonic region limit lines have been studied in great detail [2], [16], [21], and [22]. The most conspicuous property of such singularities is that two flows meet at such a line. This of course leads to a physically impossible situation, and hence the limit line may be said to imply breakdown of the continuous potential flow and signal the occurrence of a shock. It has been shown however [21], that the smooth potential flow cannot be continued beyond the limit line by simply replacing the latter by a shock.

The case $M = 1$ has been inadequately treated in the literature. The only known example of a flow with a limit line along which $M \equiv 1$ was the familiar (source) flow found by G. I. Taylor [19]. In one of the early papers on limit lines Ringleb stated erroneously that this is the only possible flow exhibiting such a limit line and that all other sonic limit singularities must occur at isolated points [16, p. 382 ff.]. Consequently sonic limit singularities have been neglected altogether and are not even discussed in textbook treatments of the subject [10] and [17].

Recently Hilda Geiringer [7] gave a new general treatment of limit lines and pointed out that limit singularities which fall along a whole non-degenerate segment of the sonic line may in fact occur in flows which have no source-like character. She called such lines <u>sonic limit lines</u>. Geiringer did not construct such a flow, but based her conclusion on a classification of sonic limit singularities in terms of the vanishing of the derivatives of the stream- and potential-function in the characteristic directions. Certain objections may however be raised about this classification (see Sec. III and the following remarks).

In a subsequent paper, Ludford and Schot [11] showed how to construct

flows containing sonic limit lines by the hodograph method and explicitly constructed a sonic limit line flow which has no source-like character*. Moreover they proved certain geometric properties of the general sonic limit line. It soon appeared that imposing the limit line condition at M = 1 singled out an interesting class of solutions which could be discussed in much more general terms.

The present thesis is an attempt to discuss as exhaustively as possible the limit singularities for the case M = 1. First we show, assuming the streamfunction to be a regular function of the hodograph variables, that a sonic limit singularity cannot be isolated but must lie either on a sonic line or on a supersonic limit line. Making use of this dichotomy we then give a new classification of sonic limit singularities which is based on the vanishing of the derivatives of the streamfunction with respect to the hodograph variables q and θ. This classification is believed to be superior to the one given by Geiringer and originally adopted by Ludford and Schot, in that it avoids the indistinctness of the characteristic variables at the sonic circle. Next we turn to a detailed discussion of the geometric properties in the neighborhood of the sonic singular point and line. The treatment of the geometry of the sonic limit line is based on Craggs' concept of an exceptional direction [2] which proved so useful in the theory of limit lines in the supersonic region. It will appear that the behavior in the neighborhood is partly different from that of the ordinary (supersonic) limit line.

In the second part we show how flows containing sonic limit lines may be constructed by forming suitable linear combinations of the Chaplygin

---

* This is the flow reproduced in Sec. X corresponding to n = 1.

product solutions of the linear hodograph equations for any value of the separation constant $n \geq 0$. This corresponds to giving certain Cauchy data along the sonic circle. For the case of general n (which may be supposed ≥ 0) the corresponding class of flows has certain well-defined geometrical features. For n less than a certain value n_0, a typical sonic limit line flow in the physical plane represents a compressible analogue of the incompressible flow about a corner (with certain corner angle), and may be envisaged as taking place on a quadruply-sheeted surface. The sheets are joined at a supersonic limit line and at the sonic limit line which has the shape of a portion of a hypocycloid ($n > 1$), cycloid ($n = 1$), or epicycloid ($n < 1$). In certain cases, portions of the same sheet overlap in the large. In addition we discuss the shape of the sonic limit line when solutions corresponding to different n are superposed and show how then the supersonic limit line can be eliminated, so that an isolated sonic limit line is obtained. An explicit flow containing such an isolated sonic limit line is constructed in Sec. XII.

In the appendix we derive the asymptotic solution for large values of n which corresponds to the sonic limit line solution. The derivation makes use of Langer's method for finding asymptotic solutions of certain ordinary differential equations in the neighborhood of a turning point [9].

II. Basic equations. We start by giving the basic equations and relations in the theory of the hodograph method which are needed in the later discussion.

The two-dimensional, steady, irrotational, isentropic flow of a compressible fluid may be described by a velocity potential $\phi(x,y)$ and

stream function $\psi(x,y)$ satisfying

$$(a^2 - u^2)\,\phi_{xx} - 2uv\,\phi_{xy} + (a^2 - v^2)\,\phi_{yy} = 0$$

(1) and

$$(a^2 - u^2)\,\psi_{xx} - 2uv\,\psi_{xy} + (a^2 - v^2)\,\psi_{yy} = 0$$

respectively, where

$$(2) \qquad u = \phi_x = \frac{1}{\rho}\psi_y\,, \qquad v = \phi_y = -\frac{1}{\rho}\psi_x$$

are the rectangular components of the velocity vector q of the flow,

$$a^2 = \frac{\gamma-1}{2}(1 - q^2)$$

is the square of the local speed of sound,

$$\rho = (1 - q^2)^{1/\gamma-1}$$

the density, and γ the adiabatic exponent of the gas.

The equations (1) can be linearized by straightforward change of the independent variables x,y to a set of polar hodograph coordinates q,θ, where q is the magnitude of the flow velocity vector, and θ its inclination relative to the x-axis. This transformation may be effected by writing (2) in the form

$$(3) \qquad \begin{aligned} d\phi &= u\,dx + v\,dy \\ \frac{1}{\rho}\,d\psi &= u\,dx - v\,dy, \end{aligned}$$

solving for dx and dy in terms of dq and $d\theta$

$$(4) \qquad \begin{aligned} dx &= \frac{1}{q}\left\{\left[\cos\theta\,\phi_q - \frac{1}{\rho}\sin\theta\,\psi_q\right]dq + \left[\cos\theta\,\phi_\theta - \frac{1}{\rho}\sin\theta\,\psi_\theta\right]d\theta\right\} \\ dy &= \frac{1}{q}\left\{\left[\sin\theta\,\phi_q + \frac{1}{\rho}\cos\theta\,\psi_q\right]dq + \left[\sin\theta\,\phi_\theta + \frac{1}{\rho}\cos\theta\,\psi_\theta\right]d\theta\right\}\,, \end{aligned}$$

and applying the integrability condition. The flow equations in the hodograph plane then become the well-known Chaplygin equations

$$(5)\qquad \begin{aligned} (M^2 - 1)\,\psi_\theta &= \rho q\, \phi_q, \\ \phi_\theta &= \frac{q}{\rho}\,\psi_q \end{aligned}$$

where the "Mach number" M has been written for the ratio q/a.

In the hyperbolic domain of the above partial differential equations (1) and (5) for ϕ and ψ one may define two families of real characteristics

$$(6)\qquad C^+ : \ \frac{dy}{dx} = \tan(\theta + \alpha), \qquad C^- : \ \frac{dy}{dx} = \tan(\theta - \alpha)$$

in the physical plane, and correspondingly

$$(7)\qquad \Gamma^+ : \ \frac{d\theta}{dq} = \frac{1}{q \tan \alpha}, \qquad \Gamma^- : \ \frac{d\theta}{dq} = -\frac{1}{q \tan \alpha}$$

in the hodograph plane, with the Mach angle $\alpha = \sin^{-1}\frac{1}{M}$. The characteristics in the hodograph plane (7) are fixed and represent the well-known Prandtl-Busemann epicycloids. If we introduce new "characteristic" coordinates $\xi(q,\theta)$, $\eta(q,\theta)$ by

$$2\xi = \int^q \frac{\sqrt{M^2 - 1}}{q}\, dq - \theta, \qquad 2\eta = \int^q \frac{\sqrt{M^2 - 1}}{q}\, dq + \theta$$

then

$$(8)\qquad \begin{aligned} \psi_\xi &= q \tan \alpha\ \psi_q - \psi_\theta \\ \psi_\eta &= q \tan \alpha\ \psi_q + \psi_\theta . \end{aligned}$$

Eliminating ϕ from the system (5) there results a differential equation for $\psi(q,\theta)$

$$(9)\qquad \psi_{qq} - \frac{(M^2 - 1)}{q^2}\,\psi_{\theta\theta} + \frac{M^2 + 1}{q}\,\psi_q = 0.$$

The general solution of equation (9) was first given by Chaplygin [1] and will be discussed in Sec. VI.

Once a solution $\psi(q,\theta)$ of Eq. (9) has been found, the coordinates x,y as functions of q,θ are given by (4). There remains the problem of inverting these functions to obtain the solution in the physical plane, namely q,θ as functions of x,y. This inversion can be carried out whenever the Jacobian of the transformation $J = \frac{\partial(x,y)}{\partial(q,\theta)}$ does not vanish. From (4) and (5)

$$J = \frac{\partial(x,y)}{\partial(q,\theta)} = \frac{\partial(x,y)}{\partial(\rho,\psi)} \cdot \frac{\partial(\rho,\psi)}{\partial(q,\theta)} = -\frac{1}{\rho^2 q^3}\left[q^2 \psi_q^2 + (1-M^2)\psi_\theta^2\right].$$

Since ρ and M are given functions of q, the points where breakdown of the mapping may occur are determined once a solution of Eq. (9) is given. Obviously when $M < 1$, J can vanish only when $\psi_q = 0$ and $\psi_\theta = 0$ which implies by (5) $\phi_\theta = 0$ and $\phi_q = 0$. It is easily seen that this can happen only at isolated points if we exclude the solution $\phi =$ constant from our discussion. However, when $M > 1$, J can vanish in general along an entire curve in the hodograph plane. Such a curve is generally called a critical curve* and its image in the flow plane is called a limit line.

A study of the hodograph mapping in a neighborhood of the limit line has been made by several authors [2], [16], [21], and [22]. Certain geometric properties may be shown always to hold at a limit line. As an example we only mention the cusping of streamlines and one family of Mach lines, the enveloping of equipotentials and the other family of Mach lines, and the fact that the acceleration of the fluid particles becomes infinite on reaching the limit line.

---

* See the footnote on p. 1.

The discussion of limit lines in the supersonic region is simplified by writing J in terms of derivatives with respect to characteristic variables ξ and η rather than with respect to q and θ. This type of treatment was first systematically applied by Geiringer [7]. Thus from (8)

$$(10) \qquad J = \frac{\partial(x,y)}{\partial(q,\theta)} = -\frac{1}{\rho^2 q^3}[q^2 \psi_q^2 + (1-M^2)\psi_\theta^2] = -\frac{1}{\rho^2 q^3}\cot^2\alpha\, \psi_\xi \psi_\eta$$

By considering the vanishing of various factors in the last member, different cases may be distinguished. Thus in the supersonic region we may differentiate between the cases $\psi_\xi = 0$, $\psi_\eta \neq 0$; $\psi_\xi \neq 0$, $\psi_\eta = 0$; and $\psi_\xi = \psi_\eta = 0$. From the implicit function theorem it may be seen that singularities of the first two kinds always occur along curves in the physical plane. Craggs calls a line in the physical plane where $\psi_\xi = 0$, $\psi_\eta \neq 0$ a limit line $\mathcal{L}_1$ and one along which $\psi_\xi \neq 0$, $\psi_\eta = 0$ a limit line $\mathcal{L}_2$.* The point of intersection of two such curves such that $\psi_\xi = \psi_\eta = 0$ is called a double limit point. (See e.g. Craggs' doublet [3].)

III. Non-isolation and classification of the sonic limit point. When $M = 1$ (i.e. $\alpha = 90^\circ$) the Jacobian J can vanish without ψ_ξ or ψ_η vanishing. In analogy with the treatment of supersonic singularities it is tempting to build up a classification of sonic limit singularities in terms of the vanishing of the factors $\cot^2\alpha$, ψ_ξ, and ψ_η in (10). This was done by Geiringer in [7] and adopted in [11]. Such a classification is not very useful however, since the characteristic directions become indistinct at the sonic circle and the derivatives ψ_ξ and ψ_η must be interpreted as limits as $M \to 1$. In many actual flow examples the behavior of these

* Their images in the hodograph plane will be denoted by ℓ_1 and ℓ_2 respectively.

quantities depends on the curve in the hodograph plane along which the sonic circle is approached*.

In this and the following sections we will present a new classification which is based on the vanishing of the derivatives of ψ with respect to q and θ where ψ is assumed to be a regular function of the hodograph variables. The main theorem proved in this section establishes that every sonic limit point must lie on some kind of limit line. This line either consists of other sonic limit points - and is then called a sonic limit line - or it consists of supersonic limit points, in which case the point is called a sonic point on a supersonic limit line. Using this dichotomy, we first examine and discuss the various singular points which may occur on a sonic limit line in Sec. IV. Besides the geometry in the neighborhood of the sonic limit line itself we discuss several types of higher-order limit points on a sonic limit line which are believed not to have been exhibited before, but occur in several of the flow examples constructed in the later sections. Sonic points on a supersonic limit line are discussed in Sec. V.

---

* For example, in Ringleb's flow [5], where

$$\psi = \frac{k}{q} \sin \theta$$

and hence from (8)

$$\psi_\xi = -\frac{k}{q}(\sin\theta \tan\alpha + \cos\theta) \qquad \psi_\eta = -\frac{k}{q}(\sin\theta \tan\alpha - \cos\theta)$$

we have that $\psi_\xi \to 0$ as $\theta^- \to 0$ and $\psi_\eta \to 0$ as $\theta^+ \to 0$ at $q = q_t$, $\theta = 0$ when these limits are approached along the branches of the supersonic limit line $\cos\theta = \pm \sin\alpha$. For all other curves of approach in the hodograph, the limits ψ_ξ and ψ_η fail to exist and one cannot classify the point $q = q_t$, $\theta = 0$ according to the above scheme.

Theorem 1: The Jacobian $J = -1/\rho^2 q^3 [\, q^2 \psi_q^2 - (M^2-1)\psi_\theta^2 \,]$ vanishes for $M = 1$ $(q = q_t)$ if and only if $\psi_q = 0$.

Proof: Clear, from the assumption that ψ and hence ψ_θ is regular.

A point at which $M = 1$, $\psi_q = 0$, $\psi_\theta \neq 0$ will be called an ordinary sonic limit point, and one at which $M = 1$, $\psi_q = 0$, $\psi_\theta = 0$ will be called a higher-order sonic limit point. It follows immediately from Chaplygin's equation that at a sonic limit point $\psi_{qq} = 0$.

A line along which $M = 1$, $\psi_q = 0$ is called a sonic limit line, $\mathcal{L}_t$. Along such a line $\psi_q = \psi_{q\theta} = \psi_{q\theta\theta} = \psi_{q\theta\theta\theta} = \dots = 0$,
$\psi_{qq} = \psi_{qq\theta} = \psi_{qq\theta\theta} = \psi_{qq\theta\theta\theta} = \dots = 0$.

Theorem 2: Every sonic point on a straight streamline is a sonic limit point.

Proof: On a straight streamline $d\psi = 0$, $d\theta = 0$, and hence
$d\psi = \psi_q dq + \psi_\theta d\theta = 0$ implies $\psi_q = 0$.

Theorem 3: A sonic limit line consisting entirely of higher-order sonic limit points does not exist.

Proof: On such a line we would have $M \equiv 1$, $\psi_q \equiv 0$, $\psi_\theta \equiv 0$ and hence $\psi(q,\theta) \equiv$ const.

Theorem 4: Every ordinary sonic limit point lies on a sonic or supersonic limit line.

Proof: At an ordinary sonic limit point $M = 1$, $\psi_q = 0$, $\psi_\theta \neq 0$ and hence

$$F = \psi_q^2 - \left(\frac{1}{a^2} - \frac{1}{q^2}\right)\psi_\theta^2 = 0$$

$$F_q = 2\psi_q\psi_{qq} - 2\psi_\theta\psi_{\theta q}\left(\frac{1}{a^2}-\frac{1}{q^2}\right) - \psi_\theta{}^2\frac{d}{dq}\left(\frac{1}{a^2}-\frac{1}{q^2}\right) = -\frac{\gamma+1}{q_t{}^3}\psi_\theta{}^2 \neq 0$$

$$F_\theta = 2\psi_q\psi_{q\theta} - 2\psi_\theta\psi_{\theta\theta}\left(\frac{1}{a^2}-\frac{1}{q^2}\right) = 0$$

and by the implicit function theorem there exists a curve $q = f(\theta)$ through the point on which $F \equiv 0$ with the direction

$$\frac{dq}{d\theta} = -\frac{F_\theta}{F_q} = 0 , \qquad q = \text{const.}$$

For higher-order sonic limit points the non-isolation of the point cannot be deduced from the implicit function theorem since $F_q = F_\theta = 0$ (and if $F_{q\theta} = 0$ then $F_{q\theta}^2 - F_{qq}F_{\theta\theta} = 0$). To handle this case we consider the sign of $F^{\pm} = \psi_q \pm (\sqrt{M^2-1}/q)\,\psi_\theta$ on certain families of curves in the neighborhood of the point.

Lemma: If at a sonic point all derivatives of ψ with respect to q and θ vanish up to and including the n'th order, then all derivatives of order n+1 vanish, except possibly $\psi_{q\underbrace{\theta\ldots\theta}_{n}}$ and $\psi_{\underbrace{\theta\theta\ldots\theta}_{n+1}}$.

Proof: This follows by successive differentiation of Chaplygin's equation (9).

Thus the discussion of the general higher-order sonic limit point where all derivatives of ψ up to and including the n'th order vanish can be broken down into the following two cases:

(a) The first (in the order of decreasing q-subscripts) non-vanishing derivative of ψ of (n+1)st order is $\psi_{\underbrace{\theta\ldots\theta}_{n+1}}$.

(b) The first non-vanishing derivative of ψ is $\psi_{q\underbrace{\theta\ldots\theta}_{n}}$.

In the second case, we have to consider n odd and n even separately.

Theorem 5: In case (a) the sonic limit point is not isolated.

Proof: Let $\frac{1}{n!}\psi_{\underbrace{\theta\theta\ldots\theta}_{n}} = \bar{k} \neq 0$. Then expanding in a neighborhood of the point*,

$$\psi_q = \mathcal{O}(\delta q, \delta\theta)^{n+1} \quad , \quad \psi_q^2 = \mathcal{O}(\delta q, \delta\theta)^{2n+2}$$

$$\psi_\theta = \bar{k}(\delta\theta)^n + \mathcal{O}(\delta q, \delta\theta)^{n+1} \quad , \quad \psi_\theta^2 = \bar{k}^2(\delta\theta)^{2n} + \mathcal{O}(\delta q, \delta\theta)^{2n+1}$$

$$\frac{M^2-1}{q^2} = \frac{\gamma+1}{q_t^3}\delta q + \mathcal{O}(\delta q)^2$$

so that

$$F = \psi_q^2 - \frac{M^2-1}{q^2}\psi_\theta^2 = -\frac{\gamma+1}{q_t^3}\bar{k}^2(\delta q)(\delta\theta)^{2n} + \mathcal{O}(\delta q, \delta\theta)^{2n+2} .$$

Thus on the straight line $\delta q = m\,\delta\theta$ through the point the principal part of F behaves as follows

$$\frac{F}{(\delta\theta)^{2n+1}} = -\frac{\gamma+1}{q_t^3}\bar{k}^2 m.$$

Thus for sufficiently small $\delta\theta \neq 0$ we have that $F \gtrless 0$ according as $\delta q = m\,\delta\theta \lessgtr 0$. This means that F takes on positive and negative values for various choices of the parameter m as shown in Fig. 1.

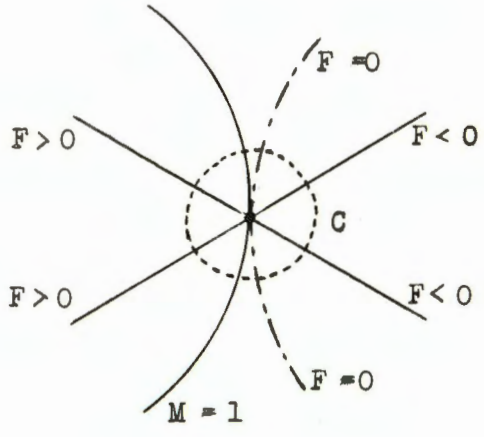

Fig. 1

Now F is a continuous function on any small circle C about the point and hence there exist points on C such that $F = 0$. Thus F must vanish on a curve through the point, and this curve cannot lie in the subsonic region,

---

* $\mathcal{O}(\delta q, \delta\theta)^n$ denotes a regular function of δq and $\delta\theta$ with terms $(\delta q)^k(\delta\theta)^\ell$ where $k + \ell \geq n$.

since limit points are isolated there.

Theorem 6: In case (b) with n odd the sonic limit point is a sonic point on a supersonic limit line.

Proof: The fact that the first nonvanishing derivative of ψ_q with respect to θ is of odd order implies by Taylor's theorem that ψ_q changes sign on $q = q_t$. This implies that the continuous function $F^+ = \psi_q + (\sqrt{M^2-1}/q)\,\psi_\theta$ tends to values with opposite signs at the ends of any sufficiently small "semicircle" C about the point on the supersonic side. (See Fig. 2.) Hence $F^+ = 0$ for some supersonic point on this semicircle. The same result holds for F^-.

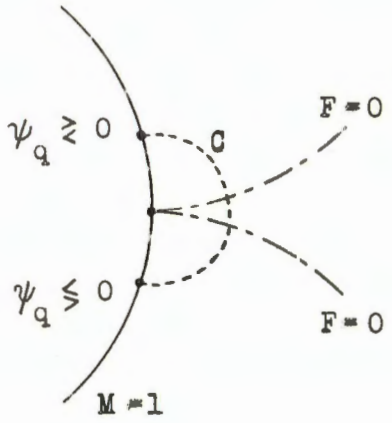

Fig. 2

Lemma: Consider case (b) with n even and the derivatives of ψ of order $1 + n + k$ at the point. Then for $k = 1,2,\ldots,n/2$,

$$(\psi_q)_{\underbrace{q\ldots q}_{n+k-p}\,\underbrace{\theta\ldots\theta}_{p}} = \begin{cases} 0 & , \quad p < n - 2k, \\ K(k)\,\psi_{q\underbrace{\theta\ldots\theta}_{n}} & , \quad p = n - 2k, \end{cases}$$

and for $k = 1,2,\ldots,n/2 - 1$,

$$(\psi_\theta)_{\underbrace{q\ldots q}_{n+k-p}\,\underbrace{\theta\ldots\theta}_{p}} = \begin{cases} 0 & , \quad p < n - 2k - 1, \\ K(k)\,\psi_{q\underbrace{\theta\ldots\theta}_{n}} & , \quad p = n - 2k - 1, \end{cases}$$

where, apart from k, K(k) depends only on the first derivative of $(1-M^2)/q^2$

at M = 1. That is, the first nonvanishing derivative of order 1 + n + k in the order of decreasing q-subscripts contains 1+3k differentiations with respect to q and is a multiple of $\psi_{q\underbrace{\theta\ldots\theta}_{n}}$ only.

Proof: Successive differentiation of Chaplygin's equation (9) shows that all derivatives of ψ of order 1 + n + k which involve more than 1+3k differentiations with respect to q can be expressed in terms of derivatives of order n and lower, and derivatives of order 1+n other than $\psi_{q\underbrace{\theta\ldots\theta}_{n}}$ and $\psi_{\underbrace{\theta\theta\ldots\theta}_{n}}$. By the previous lemma, then, these derivatives of order 1+n+k must vanish at the point.

Similarly, we see that the derivative of order 1+n+k which involves precisely 1+3k differentiations with respect to q can be expressed in terms of $\psi_{q\underbrace{\theta\ldots\theta}_{n}}$ as indicated.

It is important to note that the same results [including the function K(k)], are obtained if in Chaplygin's equation the coefficient $(1-M^2)/q^2$ is replaced by the first term in its Taylor expansion at M = 1, and the coefficient of ψ_q is replaced by zero. Thus instead of Chaplygin's equation we may consider Tricomi's equation

$$\psi_{yy} - y\,\psi_{xx} = 0, \qquad x = \theta, \quad y = \frac{\gamma+1}{3}\,\delta q \tag{11}$$

whenever we are concerned solely with the derivatives indicated in the lemma.

Theorem 7: In case (b) with n even the sonic limit point is a sonic point on a supersonic limit line.

Proof: From the lemma, the sum of the leading terms (one for each k) in the

Taylor expansion of $F^{\pm} = \psi_q \pm (\sqrt{M^2-1}/q)\ \psi_\theta$ on the semi-cubical parabola $(\sqrt[3]{(\gamma+1)/q_t^3}\,\delta q)^{3/2} = \frac{3}{2} p\ \delta\theta$ is a multiple of $\psi_{q\underbrace{\theta\ldots\theta}_{n}}$.* Now, from the remark above it is clear that the same leading terms result if Tricomi's equation (11) is used and $G^{\pm} = \psi_y \pm y^{\frac{1}{2}}\ \psi_x$ is expanded on $y^{3/2} = \frac{3}{2} p\ x$. Moreover, these leading terms remain unaltered if we construct any other solution of Tricomi's equation which gives the same $\psi_{y\underbrace{x\ldots x}_{n}}$ at the point considered and has the same earlier derivatives equal to zero there.

Now it is well known [23] that the general solution of Tricomi's equation is given by

---

* From the lemma, the principal parts of the Taylor expansions of ψ_q and ψ_θ about the point reduce to

$$\psi_q = \frac{1}{n!}\ \psi_{q\underbrace{\theta\ldots\theta}_{n}}(\delta\theta)^n + \sum_{k=1}^{k=\frac{n}{2}} \frac{1}{(n+k)!}\binom{n+k}{3k} K(k)\ \psi_{q\underbrace{\theta\ldots\theta}_{n}}(\delta q)^{3k}(\delta\theta)^{n-2k}$$

$$\psi_\theta = \frac{1}{n!}\binom{n}{1}\psi_{\theta q\underbrace{\theta\ldots\theta}_{n}}(\delta q)(\delta\theta)^{n-1} + \sum_{k=1}^{k=\frac{n}{2}-1} \frac{1}{(n+k)!}\binom{n+k}{3k+1} K(k)\ \psi_{q\underbrace{\theta\ldots\theta}_{n}}(\delta q)^{3k+1}(\delta\theta)^{n-2k-1}$$

Hence the principal part of $F^{\pm}$ on $(\sqrt[3]{(\gamma+1)/q_t^3}\ \delta q)^{3/2} = \frac{3}{2} p\ \delta\theta$ is

$$F^{\pm} = \left\{ \left[\frac{1}{n!} + \sum_{k=1}^{k=\frac{n}{2}} \frac{1}{(n+k)!}\binom{n+k}{3k}\left[(3k-1)(3k-4)\ldots 8\cdot 5\cdot 2\right]\left(\frac{3}{2}p\right)^{2k}\right] \pm \left[\frac{1}{(n-1)!}\left(\frac{3}{2}p\right) + \sum_{k=1}^{k=\frac{n}{2}-1} \frac{1}{(n+k)!}\binom{n+k}{3k+1}\left[(3k-1)\ldots 8\cdot 5\cdot 2\right]\left(\frac{3}{2}p\right)^{2k+1}\right] \right\} \psi_{q\underbrace{\theta\ldots\theta}_{n}}(\delta\theta)^n .$$

However, it is difficult to discuss changes in sign of $F^{\pm}$ from this representation.

$$\psi = \frac{\Gamma(\frac{1}{3})}{\Gamma^2(\frac{1}{6})} \int_0^1 \tau[x + \tfrac{2}{3}y^{3/2}(2t-1)]\, t^{-5/6}(1-t)^{-5/6}\,dt$$

$$+ \frac{\Gamma(\frac{5}{3})}{\Gamma^2(\frac{5}{6})}\, y \int_0^1 \nu[x + \tfrac{2}{3}y^{3/2}(2t-1)]\, t^{-1/6}(1-t)^{-1/6}\,dt$$

where

$$\tau(x) = \psi(x,0), \qquad \nu(x) = \left[\frac{\partial \psi}{\partial y}\right]_{y=0}$$

and in view of the above results we select the solution determined by the Cauchy data

$$\tau(x) = \frac{1}{n!}\,\psi_{\underbrace{yx\ldots x}_{n}}\, x^n = \alpha x^n, \qquad \nu(x) \equiv 0,$$

namely

$$\psi = \alpha \frac{\Gamma(\frac{5}{3})}{\Gamma^2(\frac{5}{6})}\, y \int_0^1 [x+\tfrac{2}{3}y^{3/2}(2t-1)]^n t^{-1/6}(1-t)^{-1/6}\,dt.$$

Forming $G^{\pm}$, we have

$$G^{\pm} = \alpha \frac{\Gamma(\frac{5}{3})}{\Gamma^2(\frac{5}{6})} \int_0^1 [x+\tfrac{2}{3}y^{3/2}(2t-1)]^{n-1} \left\{x+\tfrac{2}{3}y^{3/2}(2t-1)+ny^{3/2}[2t-1\pm 1]\right\} t^{-1/6}(1-t)^{-1/6}\,dt,$$

and on $y^{3/2} = \frac{3}{2}px$

$$G^{\pm}(p) = \alpha x^n \frac{\Gamma(\frac{5}{3})}{\Gamma^2(\frac{5}{6})} \int_0^1 [1+p(2t-1)]^{n-1}[1+p(1+\tfrac{3}{2}n)(2t-1)\pm\tfrac{3}{2}np]\, t^{-1/6}(1-t)^{-1/6}\,dt.^{*}$$

We now show that $G^{\pm}(p)$ changes sign for certain values of p. Assume that $\alpha = \frac{1}{n!}\,\psi_{\underbrace{yx\ldots x}_{n}} > 0$. Then for $p = 0$ we have

$$G^{\pm}(0) = \alpha x^n \frac{\Gamma(\frac{5}{3})}{\Gamma^2(\frac{5}{6})} \int_0^1 t^{-1/6}(1-t)^{-1/6}\,dt = \alpha x^n > 0,$$

---

* This integral is of course identical with the corresponding polynomial appearing in the previous footnote.

and for the characteristic p = 1 of the Tricomi equation

$$G^{+}(1) = \alpha x^{n} \frac{\Gamma(\frac{5}{3})}{\Gamma^{2}(\frac{5}{6})} 2^{n-1} \int_{0}^{1} [2+3nt]t^{n-7/6}(1-t)^{-1/6}dt$$

$$= \alpha x^{n} \frac{\Gamma(\frac{5}{3})\Gamma(n+\frac{5}{6})}{\Gamma(\frac{5}{6})\Gamma(n+\frac{5}{3})} 2^{n-1}(2+3n) > 0,$$

and

$$G^{-}(1) = \alpha x^{n} \frac{\Gamma(\frac{5}{3})}{\Gamma^{2}(\frac{5}{6})} 2^{n-1} \int_{0}^{1} [\,2t-3n(1-t)]t^{n-7/6}(1-t)^{-1/6}dt$$

$$= -\alpha x^{n} \frac{\Gamma(\frac{5}{3})\Gamma(n-\frac{1}{6})}{\Gamma(\frac{5}{6})\Gamma(n+\frac{5}{3})} 2^{n-2}(2+3n) < 0.$$

Similarly we have for the other characteristic p = -1,

$$G^{\pm}(-1) = \alpha x^{n} \frac{\Gamma(\frac{5}{3})}{\Gamma^{2}(\frac{5}{6})} 2^{n-1} \int_{0}^{1} [1-(1+\tfrac{3}{2}n)(2t-1) \mp \tfrac{3}{2}n]\, t^{-1/6}(1-t)^{n-7/6}dt.$$

Now letting t = 1-s

$$G^{\pm}(-1) = \alpha x^{n} \frac{\Gamma(\frac{5}{3})}{\Gamma^{2}(\frac{5}{6})} 2^{n-1} \int_{0}^{1} [1+(1+\tfrac{3}{2}n)(2s-1) \mp \tfrac{3}{2}n]\,(1-s)^{-1/6}s^{n-1/6}ds$$

so that $G^{\pm}(-1) = G^{\mp}(1)$ and hence

$G^{-}(-1) > 0$ and $G^{+}(-1) < 0$.

Thus on $y^{3/2} = \frac{3}{2}px$ the quantity $G^{\pm}$ takes on positive and negative values in the neighborhood of the point as shown in Fig. 3 and there must be at least two supersonic curves on which $G^{+} = 0$ and two supersonic curves on which $G^{-} = 0$ entering the point.

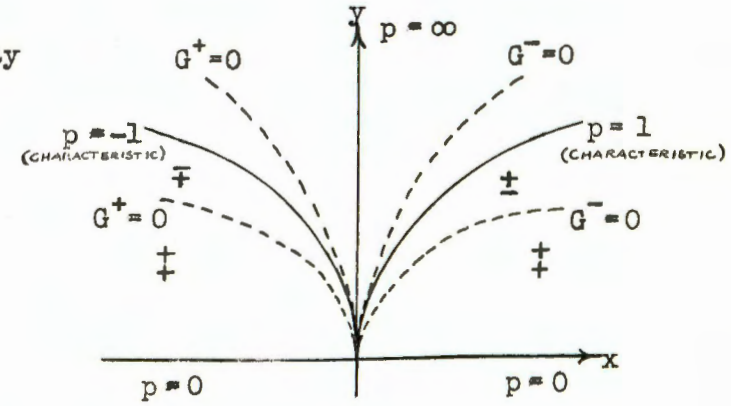

Fig. 3

With these results we can set up a classification of sonic limit (point) singularities in the hodograph method.

CLASSIFICATION OF SONIC LIMIT POINTS

(1) Point on a sonic limit line ($\psi_q \equiv 0$ on $M = 1$)

(a) Ordinary point ($\psi_\theta \neq 0$).

(b) Higher-order point ($\psi_\theta = 0$).

(i) Higher order point such that $\psi_{\theta\theta} \neq 0$.

(ii) Higher order point such that $\psi_{\theta\theta} = 0$.

(2) Point on a supersonic limit line ($\psi_q = 0$ at the point, but $\psi_q \neq 0$ in a neighborhood of the point on $M = 1$)

(a) Ordinary point ($\psi_\theta \neq 0$).

(b) Higher-order point ($\psi_\theta = 0$).

(i) First non-vanishing derivative is of the type $\psi_{\underbrace{\theta\theta..\theta}_{1+n}}$.

(ii) First non-vanishing derivative is of the type $\psi_{\underbrace{q\theta..\theta}_{1+n}}$.

IV. Point on a sonic limit line. (a) Ordinary point ($\psi_\theta \neq 0$). (Examples of such points are found in the radial flow and in the flows discussed in Sec. VI.)

Since ψ_θ can vanish only at isolated points of the sonic limit line (Theorem 3) this may be considered to be a typical point of a sonic limit line, $\mathcal{L}_t$. We show that for such a point the geometry may be discussed just as in the case of an ordinary point of the $\mathcal{L}_1$ or $\mathcal{L}_2$ in the supersonic

region, but differs from both of these.

Theorem 8: Neither an ℓ_1 nor an ℓ_2 can come into the point.

Proof: Since $\psi_q \equiv 0$ along the sonic circle $q = q_t$, we have from Taylor's formula applied to ψ_q that $\psi_q = \mathcal{O}(\delta q)$. Then $q\psi_q / \sqrt{M^2-1} = \mathcal{O}(\delta q)^{\frac{1}{2}}$, so that $\psi_\xi = (q\psi_q / \sqrt{M^2-1}) - \psi_\theta$ tends to the value $-\psi_\theta$ at $q = q_t$ irrespective of the path of approach. But if the sonic point of an ℓ_1 (on which $\psi_\xi = 0$) is approached along the ℓ_1, ψ_ξ clearly tends to zero. Hence $\psi_\theta = 0$ if such a point belongs to a sonic limit line. A similar argument holds for the ℓ_2.

The discussion of the geometry in the neighborhood of the sonic limit line is facilitated by Craggs' concept of "privileged" or "exceptional" direction [2]. An exceptional direction in our case is defined as a direction in the physical plane into which almost all directions at the corresponding point in the hodograph plane map.

Lemma: The exceptional direction at an ordinary sonic limit point is the radial direction.

Proof: From (5) and the definition of an $\mathcal{L}_t$ we have

$$\begin{cases} d\varphi = \varphi_q dq + \varphi_\theta d\theta = 0 \\ d\psi = \psi_q dq + \psi_\theta d\theta = \psi_\theta d\theta \end{cases}$$

and hence from the transformation equations (3)

$$(12) \qquad \begin{cases} dx = \frac{1}{q}\left[\cos\theta\, d\varphi - \frac{1}{\rho}\sin\theta\, d\psi\right] = -\frac{\psi_\theta}{\rho q}\sin\theta\, d\theta \\ dy = \frac{1}{q}\left[\sin\theta\, d\varphi + \frac{1}{\rho}\cos\theta\, d\psi\right] = \frac{\psi_\theta}{\rho q}\cos\theta\, d\theta\,. \end{cases}$$

Therefore

$$\frac{dy}{dx} = -\cot\theta \qquad d\theta \neq 0, \tag{13}$$

and an element of any curve in the hodograph plane on which $d\theta \neq 0$ maps into an element with slope $-\cot\theta$ in the (x,y)-plane, i.e. normal to the streamline. Next, considering the map of a curve in the hodograph plane with $d\theta = 0$ as a parameter on the corresponding curve in the physical plane we find from the transformation equations (12) that dx/dq, dy/dq vanish, but

$$\begin{cases} \dfrac{d^2x}{dq^2} = \dfrac{(\gamma-1)\cos\theta}{\rho a^5}\,\psi_\theta - \dfrac{\sin\theta}{\rho a}\,\psi_\theta\,\dfrac{d^2\theta}{dq^2} \\[2ex] \dfrac{d^2y}{dq^2} = \dfrac{(\gamma-1)\sin\theta}{\rho a^5}\,\psi_\theta + \dfrac{\cos\theta}{\rho a}\,\psi_\theta\,\dfrac{d^2\theta}{dq^2} \end{cases} . \tag{14}$$

Not both of these derivatives can vanish because the determinant of 1 and $d^2\theta/dq^2$ on the right is

$$\frac{(\gamma-1)}{\rho^2 a^6}\,\psi_\theta^2 = 0.$$

Hence the direction $d\theta = 0$ (i.e. the radial direction) is the exceptional direction and all curves in the hodograph plane having this direction map into cusped curves.

Theorem 9: The $\mathcal{L}_t$ is an equipotential and isovel, and the locus of cusps of the streamlines and isoclines. The characteristics are both tangent to the sonic line and lie on opposite sides of the isoclines (and hence streamlines). The acceleration of the fluid particles is infinite.

Proof: From Chaplygin's equations (5) $\varphi_\theta = 0$ on the sonic line, so that from $d\varphi = \varphi_\theta d\theta + \varphi_q dq = \varphi_q dq = 0$ the equipotential coincides with the isovel and both have the non-exceptional $q = \text{const.}$ direction.

For the streamlines we have $\dfrac{d\theta}{dq} = -\dfrac{\psi_q}{\psi_\theta} = 0$ and $\dfrac{d^2\theta}{dq^2} = -\dfrac{\psi_\theta\,\psi_{qq} - \psi_q\,\psi_{\theta q}}{\psi_\theta^2} = 0,$

and for the isocline $\frac{d^2\theta}{dq^2} = 0$ so that both of these have the exceptional direction and consequently map into cusped curves.

Since the characteristics C^+ and C^- are perpendicular to the streamline in the physical plane and since their images Γ^+ and Γ^- are separated by the isocline in the hodograph plane they are both tangent to the sonic limit line in the physical plane and lie on opposite sides of the isocline.

The acceleration is given by $b = q(\partial q/\partial s) = (q^2/F)\,\psi_\theta$ where s is arc length along the streamline; hence at the point $b \to \infty$.

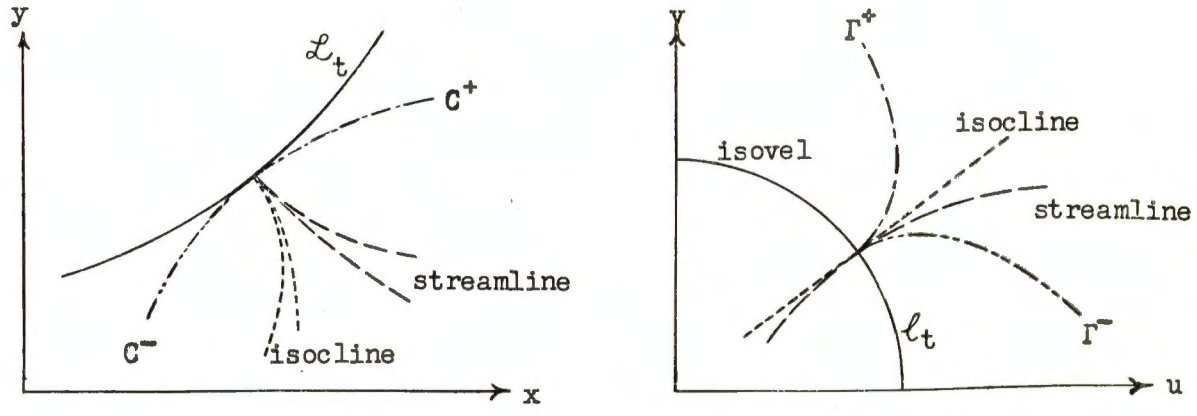

Fig. 4: Geometry in the neighborhood of the sonic limit line.

Theorem 10: If $\psi_{\theta\theta} \neq 0$, the streamline in the hodograph inflects at the point on passing from the subsonic to the supersonic region.

Proof: First we note that there is a streamline through the point. This follows from the implicit function theorem since $\psi_\theta \neq 0$ at the point.

Differentiating Chaplygin's equation (9) with respect to q and applying the conditions of an ordinary sonic limit point we have that $\psi_{qqq} \neq 0$ if (and only if) $\psi_{\theta\theta} \neq 0$. Hence using q as parameter on the streamline we find that at the point

$$\frac{d\theta}{dq} = 0, \qquad \frac{d^2\theta}{dq^2} = 0, \qquad \frac{d^3\theta}{dq^3} = -\frac{\psi_{qqq}}{\psi_\theta} \neq 0.$$

Theorem 11: Any curve in the physical plane without inflection can be a sonic limit line, the two flows which meet at it lying on the convex side.

Proof: Let the curve be denoted by $y = f(x)$ and define the stream direction θ at each point by

$$\cot \theta = - f'(x). \tag{15}$$

Considering θ as a parameter on the curve: $x = g(\theta)$, $y = h(\theta)$, we now set

$$F(\theta) = - \operatorname{cosec} \theta \, g'(\theta) = \sec \theta \, h'(\theta), \tag{16}$$

and construct the hodograph solution $\chi(q,\theta)$ which satisfies the conditions

$$\chi_q = 0, \qquad \chi_\theta = \rho_t q_t^2 F(\theta) \qquad \text{on } q = q_t.$$

Then the corresponding flow in the physical plane clearly contains a sonic limit line, whose coordinates, see (12), are given by

$$x = -\int F(\theta)\sin\theta \, d\theta = g(\theta),$$
$$y = \int F(\theta)\cos\theta \, d\theta = h(\theta),$$

when the integration constants are suitably chosen. It is easily checked that the flow is unique, except for reversal of direction, since (15) must hold at a sonic limit line (see [13]).

Consider now the map of a radial element at the sonic line in the hodograph plane. By differentiating (4), we find $dx/dq = dy/dq = 0$ and

$$\frac{d^2x}{dq^2} = \frac{(\gamma-1)\cos\theta}{\rho_t q_t^5} \chi_\theta = \frac{(\gamma-1)}{q_t^4} \cos\theta \, F(\theta) = \frac{(\gamma-1)}{q_t^4} h'(\theta),$$

$$\frac{d^2y}{dq^2} = \frac{(\gamma-1)}{q_t^4} \sin\theta \, F(\theta) = - \frac{(\gamma-1)}{q_t^4} g'(\theta),$$

where (16) has been used (cf. with the previous lemma). Hence whether the element points into the subsonic or supersonic region it maps into an element in the direction $(h'(\theta), -g'(\theta))$ perpendicular to the sonic limit line. But

according to (15): $f''(x)g'(\theta) = \operatorname{cosec}^2\theta > 0$, so that g' has the same sign as f''. Hence the image element points towards the convex side of the curve.

(b) Higher-order sonic limit point on a sonic limit line. ($\psi_\theta = 0$)

Theorem 12: Any point at which an ℓ_1, or ℓ_2, or both meet a sonic limit line is such a point.

Proof: (See Theorem 8.)

Theorem 13: Neither an ℓ_1 nor an ℓ_2 can coincide with the sonic line.

Proof: This follows from Thms. 3 and 12.

Corollary: A sonic limit line cannot be an ℓ_1 and/or ℓ_2.

(i) Higher-order sonic limit point such that $\psi_{\theta\theta} \neq 0$. (Examples of flowswith this type of singularity will be constructed in Sec. VI. These are believed to be the first examples exhibiting such a point.)

Theorem 14: An odd number of ℓ_1 and an odd number of ℓ_2 enter the point.

Proof: As in the proof of Thm. 8 we have since $\psi_q = 0$ along the sonic circle that $\psi_\xi = (q\psi_q/\sqrt{M^2-1}) - \psi_\theta$ tends to the value $-\psi_\theta$ at $q = q_t$. Now the function $\psi_\xi(q,\theta)$ is continuous on any sufficiently small supersonic "semicircle" C about the point and tends to values with opposite signs at the ends (see Fig. 5).

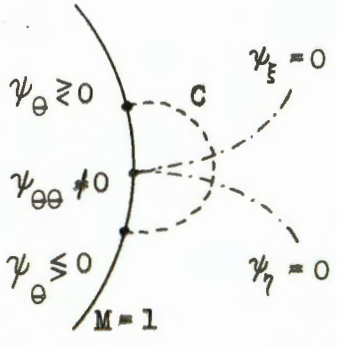

Fig. 5

Hence there exist an odd number of points on C at which $\psi_\xi = 0$. Similarly for $\psi_\eta = 0$.

Theorem 15: There is just one ℓ_1 and one ℓ_2 entering the point and together they form a cusp of the first kind* in the radial direction.

Proof: Making use of the conditions at the point $\psi_q = \psi_{\theta\theta} = \psi_{qq} = \psi_{q\theta} = 0$, $\psi_{\theta\theta} \neq 0$ (note that the sonic limit line condition is embodied in $\psi_{q\theta} = 0$), and the fact that $\psi_{\theta\theta} \neq 0$ only if $\psi_{qqq} \neq 0$ (cf. Thm. 10), we have

$$F = F_q = F_\theta = F_{qq} = F_{q\theta} = F_{\theta\theta} = F_{qqq} = F_{qq\theta} = F_{\theta\theta\theta} = 0,$$

$$F_{q\theta\theta} = -2\psi_{\theta\theta}^2\left(\frac{\gamma+1}{q_t^3}\right) \neq 0, \qquad F_{qqqq} = 6\psi_{qqq}^2 \neq 0.$$

Thus the leading terms in the Taylor expansion of the curve $F(q,\theta) = 0$ are

$$F = \frac{1}{3!}\left[3F_{q\theta\theta}(\delta q)(\delta\theta)^2\right] + \frac{1}{4!}\left[F_{qqqq}(\delta q)^4 + \ldots\right] + \ldots = 0.$$

Hence any branch enters the point either in the q-direction or in the θ-direction.

For any branch in the q-direction we may write $\delta q = x$, $\delta\theta = ux$, where u tends to zero with x, and in the x,u - plane this branch is determined by

$$G(x,u) = \frac{1}{x^3}F = \frac{1}{3!}\left[3F_{q\theta\theta}u^2\right] + \frac{1}{4!}x\left[F_{qqqq} + \ldots\right] + \ldots = 0.$$

However, since $\partial G/\partial x = F_{qqqq}/4! \neq 0$, there is a unique curve

$$x = f(u) = -12\,\frac{F_{q\theta\theta}}{F_{qqqq}}u^2 + \ldots$$

through the origin. Its image (cusp of first kind)

---

* See [5], where the method of our proof is given.

$$(\delta q)^3 = -12 \frac{F_{q\theta\theta}}{F_{qqqq}} (\delta\theta)^2 + \cdots$$

in the hodograph plane therefore provides all branches (viz. two) of $F = 0$ which enter in the radial direction.

Similarly we see that there is only one branch entering in each of the positive and negative θ-directions. These together form the sonic limit line. Thus the cusp must be formed by a unique ℓ_1 and a unique ℓ_2 (cf. Thm. 14).

Theorem 16: The sonic limit line in the physical plane is cusped at the image of the point.

Proof: From the transformation equations (4) we have along a sonic limit line (using θ as a parameter)

$$\frac{dx}{d\theta} = \frac{1}{\rho q}(-\sin\theta\ \psi_\theta), \qquad \frac{dy}{d\theta} = \frac{1}{\rho q}(\cos\theta\ \psi_\theta)$$

and

$$\frac{d^2x}{d\theta^2} = \frac{1}{\rho q}(-\cos\theta\ \psi_\theta - \sin\theta\ \psi_{\theta\theta}), \quad \frac{d^2y}{d\theta^2} = \frac{1}{\rho q}(-\sin\theta\ \psi_\theta + \cos\theta\ \psi_{\theta\theta}).$$

Hence we see that at the point both first derivatives, but not both second derivatives vanish.

Theorem 17: The streamline $\psi(q,\theta) = c$ which goes through the point in the hodograph plane has a cusp of the first kind at the point. The cusp tangent has the radial direction.

Proof: Let $\bar{\psi} = \psi - c$. Then at the point

$$\bar{\psi} = \bar{\psi}_q = \bar{\psi}_\theta = \bar{\psi}_{qq} = \bar{\psi}_{q\theta} = 0, \quad \bar{\psi}_{\theta\theta} \neq 0 \quad \text{and hence} \quad \bar{\psi}_{qqq} \neq 0$$

(cf. Thm. 10). The Taylor expansion of $\bar{\psi}$ about the point is

$$\bar{\psi} = \frac{1}{2!}\left[\bar{\psi}_{\theta\theta}(\delta\theta)^2\right] + \frac{1}{3!}\left[\bar{\psi}_{qqq}(\delta q)^3 + \ldots\right] + \ldots$$

Thus according to [5] it can be seen that the curve $\bar{\psi}(q,\theta)$ forms a single cusp of the first kind with cusp tangent in the radial direction.

(ii) Higher order sonic limit point such that $\psi_{\theta\theta} = 0$. (An example of a flow with this type of singularity will be presented in Sec. XII.)

There exist cases where no supersonic limit line enters the point. A necessary condition in this case (cf. Thm. 14) is that ψ_θ does not change sign on $q = q_t$. An example is presented in Sec. XII.

The sonic limit line need not be cusped at the image point in the physical plane. From the proof of Thm. 16 we see that at the point $dx/d\theta = dy/d\theta = d^2x/d\theta^2 = d^2y/d\theta^2 = 0$, but if $\psi_{\theta\theta\theta} \neq 0$ then not both third derivatives vanish.

Theorem 18: If a supersonic limit line enters the point in the hodograph, it is either perpendicular or tangent to the sonic limit line.

Proof: Since the point lies on a sonic limit line, the first nonvanishing derivative must be of the type $\psi_{\underbrace{\theta\ldots\theta}_{1+n}} \neq 0$ (see Sec. III). Then the expansion of Thm. 5 holds

$$F = -\frac{\gamma+1}{q_t^3}\bar{k}^2(\delta q)(\delta\theta)^{2n} + \delta(\delta q, \delta\theta)^{2n+2}$$

and the curve on which $F(q,\theta) = 0$ is either tangent ($\delta q = 0$) or perpendicular ($\delta\theta = 0$) to the sonic circle.

Theorem 19: If $\psi_{\theta\theta\theta} \neq 0$, then the streamline $\psi(q,\theta) = c$ through the point has a triple point with three branches entering from the subsonic side, and one from the supersonic side, all in the radial direction. Two of the branches on the subsonic side form a cusp of the first kind.

Proof: As in Thm. 17, let $\bar{\psi} = \psi - c$. Then at the point

$$\bar{\psi} = \bar{\psi}_q = \bar{\psi}_\theta = \bar{\psi}_{qq} = \bar{\psi}_{q\theta} = \bar{\psi}_{\theta\theta} = \bar{\psi}_{qqq} = \bar{\psi}_{qq\theta} = \bar{\psi}_{q\theta\theta} = 0,$$

$$\bar{\psi}_{\theta\theta\theta} \neq 0, \quad \bar{\psi}_{qqqq} = 0, \quad \bar{\psi}_{qqq\theta} = -\frac{\gamma+1}{q_t^3}\bar{\psi}_{\theta\theta\theta} \neq 0, \quad \bar{\psi}_{qqqqq} = 0,$$

and the Taylor expansion about the point is

$$\bar{\psi} = \frac{1}{3!}\left[\bar{\psi}_{\theta\theta\theta}(\delta\theta)^3\right] + \frac{1}{4!}\left[\binom{4}{1}\bar{\psi}_{qqq\theta}(\delta q)^3(\delta\theta)\right] + \cdots$$

$$+ \frac{1}{5!}\left[\binom{5}{1}\bar{\psi}_{qqqq\theta}(\delta q)^4(\delta\theta) + \cdots\right] + \cdots .$$

Thus any branch of the curve $\bar{\psi}(q,\theta) = 0$ coming into the point has the direction $\delta\theta = 0$. Now let $b = 3!\,\bar{\psi}_{qqq\theta}/\bar{\psi}_{\theta\theta\theta} = -3!(\gamma+1)/q_t^3 < 0$ and $b' = 3!\,\bar{\psi}_{qqqq\theta}/\bar{\psi}_{\theta\theta\theta}$ and put $\delta\theta = ux$, $\delta q = x$. Then

$$G(x,u) = \frac{3!\,\bar{\psi}}{\bar{\psi}_{\theta\theta\theta}} \cdot \frac{1}{x^3} = u^3 + x[bu + \cdots] + x^2[b'u + \cdots] + \cdots = 0$$

and the curve $G(x,u) = 0$ enters along $bux = 0$, i.e. $x = 0$ or $u = 0$.

By repeating the argument as in the proof of Thm. 14, we find that the branch $x = 0$ corresponds to a unique curve, whose image in the hodograph

$$(\delta\theta)^2 = -b(\delta q)^3 + \cdots$$

forms a cusp of the first kind. Since $b < 0$, this branch falls on the subsonic side of the sonic circle.

By a similar analysis, the branch $u = 0$ may be shown to correspond to

a unique curve, whose image in the hodograph passes through the point in the radial direction.

V. Sonic point of a supersonic limit line. (a) Ordinary point ($\chi_\theta \neq 0$)

(Examples of such a point are found in the flows of Ringleb and of Temple and Yarwood. See e.g. [13].)

Theorem 20: The supersonic limit line is unique and is tangent to the sonic circle at the point.

Proof: As in Thm. 4, we have at the point: $F = F_\theta = 0$, $F_q \neq 0$. Hence there is a unique line $q = f(\theta)$ through the point on which $F(q,\theta) \equiv 0$ and it has the direction

$$\frac{dq}{d\theta} = -\frac{F_\theta}{F_q} = 0, \qquad q = \text{const.}$$

Theorem 21: The geometry at the point in both physical and hodograph planes is the same as for an ordinary point of a sonic limit line.

Proof: The directions of the isovel, equipotential, characteristics, streamline and isocline in the hodograph plane depend only on the property $\chi_q = 0$, $\chi_\theta \neq 0$ at the point. Moreover the effect on these curves of the mapping from the hodograph into the physical plane depends only on $\chi_q = 0$, $\chi_\theta \neq 0$ at the point. (Cf. Thm. 9 and [2].)

(b) Sonic point of a supersonic limit line: Higher-order point ($\chi_\theta = 0$)

(i) First nonvanishing derivative is of the type $\chi_{\underbrace{\theta\ldots\theta}_{1+n}} \neq 0$. (The simplest example of this type of flow is one where $n = 1$, i.e. at the point:

$\psi_q = \psi_\theta = \psi_{qq} = \psi_{q\theta} = 0$, $\psi_{\theta\theta} \neq 0$. Such a flow can be constructed by superposition of Chaplygin solutions as follows:

$$\psi = A\theta + B\int \frac{\rho}{q}\,dq + \frac{1}{q}(\sin\theta + \cos\theta) + CF_2(q)\sin 2\theta$$

where $F_2(q) = q^2F(\frac{5}{3},-3,3,q^2)$, $A = -[q_tF_2'(q_t) + F_2(q_t)]\,/q_t^2F_2'(q_t)$, $B = 1/\rho_t q_t$, and $C = 1/2q_t^2F_2'(q_t)$.)

Theorem 22: The branches of the supersonic limit line come into the point tangentially or perpendicularly to the sonic circle.

Proof: As in Thm. 5 the Taylor expansion of F about the point is

$$F = -\frac{\gamma+1}{q_t^3}\bar{k}^2(\delta q)(\delta\theta)^{2n} + \mathcal{O}(\delta q,\delta\theta)^{2n+2}$$

hence the curve on which $F \equiv 0$ has the direction $\delta q = 0$ and/or $\delta\theta = 0$.

(ii) First nonvanishing derivative (q decreasing) is of the type $\psi_{\underbrace{q\theta\ldots\theta}_{1+n}} \neq 0$.

(The simplest example of this type of flow is one where $n = 1$, i.e. $\psi_q = \psi_\theta = \psi_{qq} = 0$, $\psi_{q\theta} \neq 0$. Such a point is $q = q_t$, $\theta = 0$ in the flow $\psi = k\theta + (1/q)\sin\theta$, where $k = -1/q_t$.)

Theorem 23: The branches of the supersonic limit line come into the point perpendicularly.

Proof: Let $\frac{1}{n!}\psi_{\underbrace{q\theta\ldots\theta}_{1+n}} = k' \neq 0$. Then as in Thm. 5 we find the Taylor series of F about the point

$$F = k'^2(\delta\theta)^{2n} + \mathcal{O}(\delta q,\delta\theta)^{2n+1}.$$

Hence $F \equiv 0$ has the direction $\delta\theta = 0$.

VI. Sonic limit line flows for any n. The only known flow involving a sonic limit line is the radial (or "source") flow. We will presently show how more general examples of flows with an $\mathscr{L}_t$ may be constructed by forming certain linear combinations of solutions of Chaplygin's equation (9).

The discussion of the flow corresponding to a particular solution of the hodograph equation is facilitated by introducing the variable $\tau = q^2$ in place of q. With this variable Chaplygin's equations (5) take the form

$$\varphi_\theta = 2\tau(1-\tau)^{-\beta}\,\psi_\tau$$

(17)

$$[1-(1+2\beta)\tau]\,\psi_\theta = -2\tau(1-\tau)^{\beta+1}\varphi_\tau$$

where $\beta = 1/(\gamma-1)$. On eliminating φ we have, in place of (9),

$$2\tau(1-\tau)^{\beta+1}\frac{\partial}{\partial\tau}\left[2\tau(1-\tau)^{-\beta}\frac{\partial\psi}{\partial\tau}\right]+[1-(1+2\beta)\tau]\frac{\partial^2\psi}{\partial\theta^2}=0.$$

One solution of this equation is the radial (source) flow $\psi = k\theta$ discussed by G. I. Taylor [19]. Other solutions may be obtained by the method of separation of variables:

(18) $$\psi_n(\tau,\theta) = P_n(\tau)\sin n\theta = \tau^{\frac{n}{2}}H_n(\tau)\sin n\theta$$ *

where $H_n(\tau)$ is, in general, a combination of hypergeometric functions, **

(21) $$H_n(\tau) = \lambda_n F_n^{(1)}(\tau) + \tau^{-n}F_n^{(2)}(\tau)$$

---

* In general $\psi(\tau,\theta) = P_n(\tau)\sin(n\theta+\varepsilon_n) = \tau^{\frac{n}{2}}H_n(\tau)\sin(n\theta+\varepsilon_n)$. Since the inclusion of the phase angle ε_n merely amounts to a rotation of axes in the physical plane, there is no loss in generality in taking ε_n to be zero throughout the following discussion.

** $F_n^{(1)}(\tau)$ is the hypergeometric function

(19) $$F_n^{(1)}(\tau) = F(a_n,b_n,n+1;\tau) = \frac{\Gamma(n+1)}{\Gamma(a_n)\Gamma(b_n)}\sum_{n=0}^{\infty}\frac{\Gamma(a_n+k)\Gamma(b_n+k)}{\Gamma(n+1+k)}\cdot\frac{\tau^k}{k!}$$

with $a_n+b_n = n-\beta$, $a_nb_n = -\frac{n(n+1)}{2}\beta$. The function $F_n^{(2)}(\tau)$ is given by

(20) $$F_n^{(2)}(\tau) = F(a_n-n,b_n-n,-n+1;\tau)$$

whenever $n \neq 0,-1,-2,\ldots$. When the index n is integral and negative however, the solution $\tau^{-n}F_n^{(2)}(\tau)$ with $F_n^{(2)}(\tau)$ given by (20) is in general not linearly independent from $F_n^{(1)}(\tau)$, and $F_n^{(2)}(\tau)$ must be replaced by a logarithmic term [6].

satisfying the equation

$$(22) \qquad \tau(1-\tau)H_n'' + [(n-1) - (n+1-\beta)\tau]H_n' + \tfrac{1}{2}n(n+1)\beta H_n = 0,$$

primes indicating differentiation with respect to τ.

For any positive real number n, a solution containing a sonic limit line can be obtained by choosing the constant λ_n in the combination so that

$$(23) \qquad \frac{dP_n}{d\tau} = \frac{d}{d\tau}[\tau^{\frac{1}{2}}H_n(\tau)] = 0 \qquad \text{at the sonic value} \quad \tau = \tau_t = \frac{1}{2\beta+1} \ .$$

For then $\partial\psi_n/\partial q \equiv 0$ for all $q = 1/\sqrt{2\beta+1} = q_t$. Since the equation (22) is linear, any linear combination of such solutions (21) will also be a solution containing a sonic limit line. The discussion of these composite flows will be deferred until Sec. XI.

Corresponding to this solution in the τ,θ - plane, the coordinate functions, from (4), (5), and (18), are given parametrically in terms of τ and θ by *

$$(24) \qquad \begin{cases} x_n = \frac{1}{2}\tau^{-\frac{1}{2}}(1-\tau)^{-\beta}\left[-\frac{1}{n+1}(2\tau\frac{dP_n}{d\tau} - nP_n)\cos(n+1)\theta - \frac{1}{n-1}(2\tau\frac{dP_n}{d\tau} + nP_n)\cos(n-1)\theta\right] \\ y_n = \frac{1}{2}\tau^{-\frac{1}{2}}(1-\tau)^{-\beta}\left[-\frac{1}{n+1}(2\tau\frac{dP_n}{d\tau} - nP_n)\sin(n+1)\theta + \frac{1}{n-1}(2\tau\frac{dP_n}{d\tau} + nP_n)\sin(n-1)\theta\right] \end{cases}$$

if $n \neq 1$, and in the case $n = 1$

$$(25) \qquad \begin{cases} x_1 = \frac{1}{2}\tau^{-\frac{1}{2}}(1-\tau)^{-\frac{5}{2}}\left[-\frac{1}{2}(2\tau\frac{dP_1}{d\tau} - P_1)\cos 2\theta\right] + f(\tau) \\ y_1 = \frac{1}{2}\tau^{-\frac{1}{2}}(1-\tau)^{-\frac{5}{2}}\left[-\frac{1}{2}(2\tau\frac{dP_1}{d\tau} - P_1)\sin 2\theta + (2\tau\frac{dP_1}{d\tau} + P_1)\theta\right] \end{cases}$$

where

$$f(\tau) = -\frac{1}{8}\int\tau^{-\frac{1}{2}}(1-\tau)^{\beta}\left[3P_1 - \frac{2\beta\tau}{1-\tau}P_1' - 8\tau P''\right]d\tau \ .$$

---

* deleting the non-essential constants of integration

The case $n = 0$, leading to the well-known radial flow will be omitted in the discussion.

We now investigate the shape of the sonic limit line in the physical plane corresponding to any $n > 0$. From (23), (24), and (25) it is given by

$$(26)\qquad \begin{cases} x_n = \dfrac{nP_n(\tau_t)}{2\tau_t^{\frac{1}{2}}(1-\tau_t)^{\beta}}\left[\dfrac{1}{n+1}\cos(n+1)\theta - \dfrac{1}{n-1}\cos(n-1)\theta\right], \\ y_n = \dfrac{nP_n(\tau_t)}{2\tau_t^{\frac{1}{2}}(1-\tau_t)^{\beta}}\left[\dfrac{1}{n+1}\sin(n+1)\theta + \dfrac{1}{n-1}\sin(n-1)\theta\right] \end{cases}$$

if $n \neq 1$, and in the case $n = 1$

$$(27)\qquad \begin{cases} x_1 = \dfrac{P_1(\tau_t)}{4\tau_t^{\frac{1}{2}}(1-\tau_t)^{\frac{5}{2}}}[\cos 2\theta] + f(\tau_t) \\ y_1 = \dfrac{P_1(\tau_t)}{4\tau_t^{\frac{1}{2}}(1-\tau_t)^{\frac{5}{2}}}[\sin 2\theta + 2\theta]. \end{cases}$$

These are the parametric equations of curves (roulettes) which can be generated by rolling a circle on the outside or inside of a fixed circle. For $n > 1$ the ratio of the radius of the rolling circle to that of the fixed circle is $(n-1)/2n$ and the curves are hypocycloids. For $n < 1$ this ratio is $(1-n)/2n$ and the curves are epicycloids. For $n = 1$ the curve is a cycloid and for $n = 0$ (the radial flow) the roulette degenerates into a circle. When $2n/(n-1)$ is rational, the sonic limit line will close up after a certain number of revolutions. Thus for $n = \frac{1}{3}, \frac{1}{2}, 2, 3$ the curves are particularly simple, namely a cardioid, nephroid, astroid, and tricuspid, respectively.

In Sec. IV we called a point where $\psi_\tau = \psi_\theta = 0$ for $\tau = \tau_t$ a higher-order sonic limit point. Thus for any n, the sonic limit line will have higher-order sonic limit points where

$$\psi_\theta = \tau_t^{\frac{n}{2}} H_n(\tau_t) \cos n\theta = 0,$$

that is, at the points corresponding to

$$\theta = \frac{2m+1}{n}\cdot\frac{\pi}{2} \qquad m = 0, \pm 1, \pm 2, \ldots . \tag{28}$$

It is precisely at these points that the roulettes have their cusps. The general sonic limit line does not necessarily have cusps at its higher-order sonic limit points, however. This depends on the vanishing of $\psi_{\theta\theta}$ (cf. Sec. IV).

VII. The associated supersonic limit line and streamlines in the hodograph. In addition to the desired sonic limit lines the flows given by (18) also possess other (nonsonic) limit singularities (cf. Theorem 14). The Jacobian of the transformation from the hodograph to the physical plane shows that these occur where

$$\frac{\partial(x,y)}{\partial(\tau,\theta)} = -\frac{2\tau}{(1-\tau)^\beta}\left(\frac{\partial\psi}{\partial\tau}\right)^2 + \frac{(2\beta+1)\tau-1}{2\tau(1-\tau)^{\beta+1}}\left(\frac{\partial\psi}{\partial\theta}\right)^2 = 0. \tag{29}$$

For the solutions (18) these (supersonic) limit lines are the curves

$$\cot n\theta = \mp\sqrt{\frac{1-\tau}{(2\beta+1)\tau-1}}\cdot\frac{2\tau}{n}\cdot\frac{1}{P_n}\cdot\frac{dP_n}{d\tau} . \tag{30}$$

To investigate the shape of these curves we note from (22) that the function $P_n(\tau)$ satisfies the equation

$$\frac{d}{d\tau}\left[\frac{\tau}{(1-\tau)^\beta}\frac{dP_n}{d\tau}\right] - \frac{n^2}{4}\cdot\frac{1-(2\beta+1)\tau}{\tau(1-\tau)^{\beta+1}}P_n = 0. \tag{31}$$

Hence if we let

$$S_n = \frac{2\tau}{n}\cdot\frac{1}{P_n}\cdot\frac{dP_n}{d\tau} \quad , \tag{32}$$

then S_n will satisfy the Riccati equation

$$\frac{dS_n}{d\tau} + \frac{\beta}{1-\tau}S_n + \frac{n}{2\tau}\left[S_n^2 - \frac{1-(2\beta+1)\tau}{1-\tau}\right] = 0. \tag{33}$$

At the sonic circle $\tau = \tau_t = \frac{1}{2\beta+1}$ we have the conditions

$$S_n = 0, \qquad \frac{dS_n}{d\tau} = 0 \tag{34}$$

which follow from (23) and (33).

Now the expression on the right of (30) becomes indeterminate at $\tau = \tau_t$, but application of L'Hospital's rule leads to

$$\cot n\theta = 0, \quad \theta = \frac{2m+1}{n}\cdot\frac{\pi}{2} \qquad m=0,\pm1,\pm2,\ldots \ . \tag{35}$$

Hence the supersonic limit line intersects the sonic limit line at the higher-order sonic limit points. This was shown to be a general property of sonic limit lines in Theorem 12. Moreover it was shown in Theorem 15 that, when $\psi_{\theta\theta} \neq 0$, the supersonic limit line enters the higher-order sonic limit point in a cusp. At the maximum circle $\tau = 1$, again (35) holds. For $(2m/n)(\pi/2) < \theta < [(2m+2)/n](\pi/2)$ the supersonic limit line must extend from $\tau = \tau_t$ to $\tau = 1$, in two symmetric branches (corresponding to the plus and minus signs in (30)) about the line of symmetry $\theta = [(2m+1)/n](\pi/2)$.

In order to determine the number of sheets required to represent the flow in the physical plane it is important to know whether the branches of the supersonic limit line in the hodograph plane intersect again on the line $\theta = [(2m+1)/n](\pi/2)$ in the interval $\tau_t < \tau < 1$. Such supersonic double limit points certainly occur for some combinations of $F^{(1)}(\tau)$ and $F^{(2)}(\tau)$

(see for example Cragg's doublet [3]). We shall show, however, that for any n less than a certain value n_0, which we don't compute explicitly, the flow represented by (21), does not possess such supersonic double limit points.

From (30) and (32) such a double limit point would have to occur at a zero of S_n. Now at the initial point τ_t of the interval $\tau_t \leq \tau \leq 1$ we have, on differentiating (33) and using (34), that

$$\frac{d^2S_n}{d\tau^2} = -\frac{n(2\beta+1)}{2\tau(1-\tau)^2} < 0,$$

so that from (34), $S_n(\tau)$ is negative in the neighborhood of τ_t. Thus if the curve $S_n = S_n(\tau)$ were continuous in the interval $\tau_t < \tau < 1$, it could never cross or touch the τ-axis in this interval, for it would have to do so with non-negative slope and from (33) we see that at a zero of S_n in the supersonic region $dS_n/d\tau$ would have to be negative.

We now investigate the possibility that $S_n = S_n(\tau)$ has an infinity in the interval $\tau_t < \tau < 1$. Consider the zero isoclines of (33). The ordinates of these isoclines are given from (33) by

$$S_n = \frac{-\beta\tau \pm \sqrt{\beta^2\tau^2 - n^2(1-\tau)[(2\beta+1)\tau - 1]}}{n(1-\tau)}$$

and are real when

$$\Delta = \beta^2 - n^2\left(\frac{1}{\tau} - 1\right)\left(2\beta+1-\frac{1}{\tau}\right) \geq 0.$$

Now the maximum of $(1/\tau - 1)(2\beta+1-1/\tau)$ occurs at $\tau = 1/\beta + 1$ and is β^2.

Hence for any $n \leq 1$, we have $\Delta \geq 0$ and the zero isoclines extend from $\tau = 0$ to $\tau = 1$ and have non-positive slope. From the sketch (Fig. 6) it is clear that the integral curve $S_n(\tau)$ which satisfies the conditions (34) at $\tau = \tau_t$ cannot have a singularity in the range $\tau_t < \tau < 1$, for it must lie below the τ-axis and cannot cross the zero isoclines which bound it from

below. Thus $S_n < 0$ for all $\tau_t < \tau < 1$.

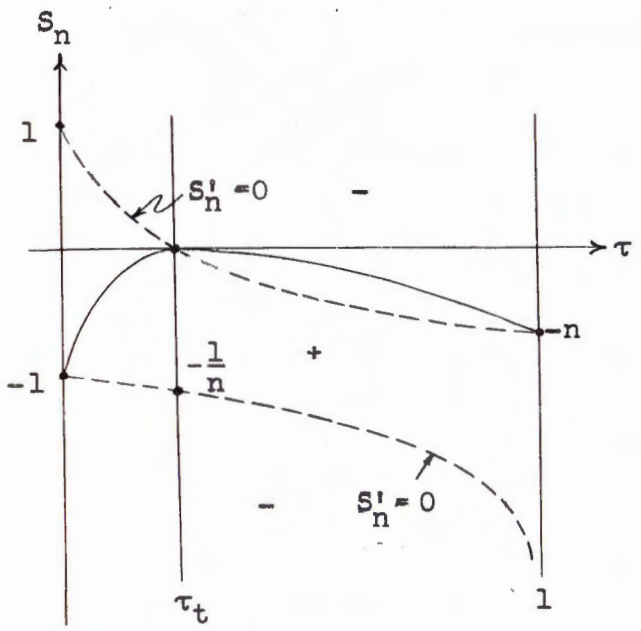

Fig. 6: $n<1$

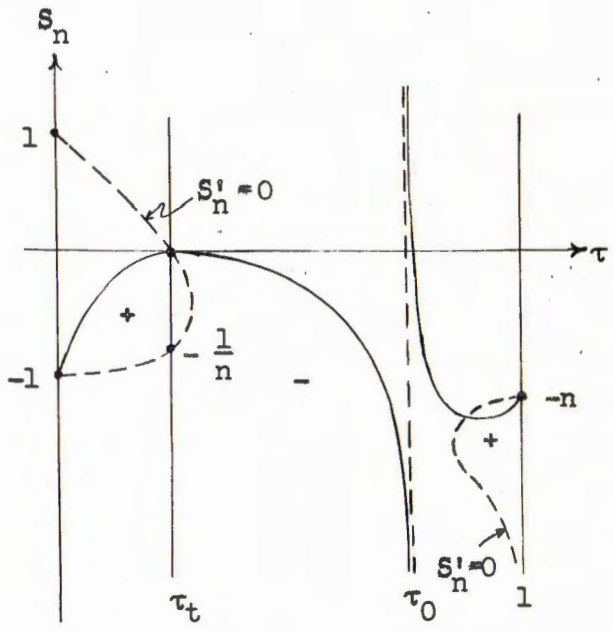

Fig. 7: $1<n_0<n$

Consider now the case $n > 1$. For $n > 1$, we have $\Delta < 0$, and the zero isocline split up into two branches as shown in Fig. 7. Thus the integral curve $S_n(\tau)$ which satisfies (34) is no longer "bounded from below" by the isoclines, but could have a singularity at some point τ_0 in the interval $\tau_t < \tau < 1$ such that $\lim_{\tau \to \tau_0^-} S_n(\tau) = -\infty$ and $\lim_{\tau \to \tau_0^+} S_n(\tau) = +\infty$. As shown in the figure, the branch on which $\lim_{\tau \to \tau_0^+} S_n(\tau) = +\infty$ will then cross the τ-axis with negative slope, as required by (33).

It can be shown from the asymptotic behavior of (33) that such infinities do in fact occur for large values of n. If we let n_0 be the smallest value of n for which our integral curve first has a singularity, then it will have singularities (and hence zeroes) for all n greater than n_0.

---

*The plus and minus signs indicate regions in which the integral curves have positive and negative slope, respectively.

The value n_0 for which $S_n(\tau)$ first has zeroes will not be calculated explicitly. However, the example worked out in section IX for the case $n = 2$ exhibits no supersonic double limit points, so that we may conclude $n_0 > 2$.

From these results it is clear then, that for any $n < n_0$ the supersonic limit line in the hodograph plane in a flow given by (18) consists for $(2m/n)(\pi/2) < \theta < [(2m+2)/n](\pi/2)$ of a drop-shaped portion with the line $\theta = [(2m+1)/n](\pi/2)$ as axis of symmetry (see for example Fig. 9). We will not discuss the shape of the supersonic limit line when $n \geq n_0$.

We now turn to a discussion of the streamlines in the hodograph plane for the case $n < n_0$. The straight streamlines are given by $d\psi = \psi_\tau d\tau + \psi_\theta d\theta = 0$, $d\theta = 0$ which implies $\psi_\tau = 0$. From the expression for the streamfunction (18) we see that this implies

$$\theta = m\cdot\frac{\pi}{n}, \qquad m=0,\pm1,\pm2,\ldots .$$

By symmetry we need only consider the circular sector $0 < \theta < \pi/n$. By interpreting the straight streamlines as boundaries in the physical plane it is evident that (18) represents flow about a corner of angle $\pi-(\pi/n)$. The total angle through which the stream turns is π/n.

Let us now consider the non-straight streamlines in the hodograph. Differentiating (18) along a streamline

$$d\psi = \frac{dP_n}{d\tau}\sin n\theta\, d\tau + nP_n\cos n\theta\, d\theta = 0,$$

so that the inclination α of the streamline to the radius vector at any point of the hodograph is given by

$$\cot\alpha = \frac{1}{2\tau}\cdot\frac{d\tau}{d\theta} = -\frac{\cot n\theta}{2\tau}\cdot\frac{P_n}{P_n'}$$

and on substituting (18) we find

$$\cot\alpha = -\frac{\cot n\theta}{S_n}. \tag{36}$$

Now we have seen above that

$$S_n = 0 \quad \text{at} \quad \tau = \tau_t \; ; \qquad S_n < 0 \quad \text{throughout} \quad \tau_t < \tau < 1.$$

By a similar argument to that in the proof above, it can be shown that

$$S_n < 0 \quad \text{throughout} \quad 0 < \tau < \tau_t$$

so that for $n < n_0$,

$$\text{sign } (\cot \alpha) = \text{sign } (\cot n\theta) \qquad \text{throughout} \quad 0 < \tau < 1.$$

Since all streamlines pass through the origin, it is clear then, that as θ increases from 0 to π/n the streamlines traverse a closed loop, which is symmetric about the line $\theta = \pi/2n$ (see e.g. Fig. 9). The curvature of the streamlines changes continuously as this loop is traversed, and becomes zero at the sonic circle $\tau = \tau_t$ (in accord with the theory of the sonic limit line, Sec. IV and Theorem 9). The only exception to this general behavior of the non-straight streamlines is the streamline, say ψ_c, which passes through the higher-order sonic limit point at $\tau = \tau_t$, $\theta = \pi/2n$. This streamline is given by

$$\psi_c = P_n(\tau_t) \sin n\left(\frac{\pi}{2n}\right) = P_n(\tau_t)$$

and is known to have a cusp at that point (Theorem 17). It divides the streamlines which do not intersect a limit line (sonic or supersonic) from those that do, and will be called the critical streamline ψ_c. Another streamline of interest is the one passing through the point $\tau = 1$, $\theta = \pi/2n$. We will call this streamline, given by

$$\psi_a = P_n(1) \sin n\left(\frac{\pi}{2n}\right) = P_n(1),$$

the asymptotic streamline, for reasons which will become clear in the next section.

The streamlines in the hodograph plane may then be divided into three

classes:

(a) those which intersect neither the ℓ_t nor the ℓ : $\psi_c < \psi < \infty$,

(b) those which intersect both the ℓ_t and the ℓ : $\psi_a < \psi < \psi_c$,

(c) those which intersect only the ℓ_t : $0 < \psi < \psi_a$.

The behavior of these three types of streamlines in the physical plane is radically different.

VIII. The physical plane. Consider now the flow in the physical plane corresponding to the hodograph flow in the typical circular sector $0 < \tau < 1$, $0 < \theta < \pi/n$. From the geometry in the neighborhood of the limit line (sonic and supersonic) we know that the streamlines are cusped at the limit line and consequently the region to one side of the limit line becomes multiply covered. Thus the limit lines in the physical plane delineate regions in which the flow changes its multi-valued character (cf. [9] and [15]). This can be envisaged as a folding of the physical plane into a multiply-sheeted configuration, with folds at the limit lines so that each sheet is simply covered by the appropriate portion of the total flow, and at the limit line folds, the flow passes from one sheet to the appropriate next sheet. Due to our choice of the representative circular sector in the hodograph the entire multi-sheeted configuration representing the physical plane is of course bounded by the map of the sides of the sector, i.e. the straight streamlines $\theta = 0$, $\theta = \pi/n$.

We have already discussed the shape of the sonic limit line in the physical plane. The supersonic limit line maps into a wedge-shaped curve with a cusp at the higher-order sonic limit point, the cusp direction coinciding with that of the sonic limit line.

The physical plane must thus be envisaged as a quadruply-sheeted

surface, the sheets corresponding to the regions in the hodograph bounded by (see Fig. 8):

(I) $0 < \tau < \tau_t$, $\theta = 0$; $\tau = \tau_t$, $0 < \theta < \frac{\pi}{n}$; $0 < \tau < \tau_t$, $\theta = \frac{\pi}{2n}$;

(II) $\tau_t < \tau < 1$, $\theta = 0$; $\tau = 1$, $0 < \theta < \frac{\pi}{2n}$; ℓ_1; $\tau = \tau_t$, $0 < \theta < \frac{\pi}{2n}$;

(III) ℓ_1 ; ℓ_2 ;

(IV) ℓ_2 ; $\tau = 1$, $\frac{\pi}{2n} < \theta < \frac{\pi}{n}$; $\tau_t < \tau < 1$, $\theta = \frac{\pi}{n}$; $\tau = \tau_t$, $\frac{\pi}{2n} < \theta < \frac{\pi}{n}$.

The examples in Secs. IX and X show that portions of sheet I may overlap.

The streamlines in the physical plane behave as follows. Initially all streamlines have the $\theta = 0$ direction. They then bend around in a clockwise direction and finally all assume the $\theta = \pi/n$ direction. Between these two final states their behavior depends on the group to which they belong in our classification of streamlines in the hodograph plane:

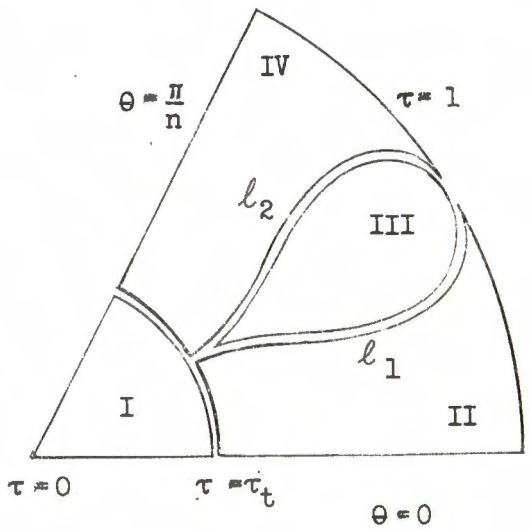

Fig. 8

(a) These streamlines bend smoothly about the cusp of the $\mathcal{L}_t$ and never leave sheet I.

(b) These start on sheet I, are cusped at the $\mathcal{L}_t$ and pass onto sheet II, continue on sheet II until they meet the $\mathcal{L}_1$, reflect onto sheet III, continue on sheet III until they reach the $\mathcal{L}_2$, pass there to sheet IV, continue on sheet IV up to the $\mathcal{L}_t$, and reflect back onto sheet I.

(c) These start on sheet I, reflect at one branch of the $\mathscr{L}_t$ onto sheet II and continue on this sheet to infinity (the circle $\tau = 1$ maps into infinity in the physical plane), they then return on sheet IV, and reflect at the other branch of the $\mathscr{L}_t$ back onto sheet I.

Note that the dividing streamline between group (b) and group (c), namely ψ_a, asymptotically approaches the two branches of the supersonic limit line.

Examples having the features described above are worked out in the next two sections.

IX. The sonic limit line flows for $n = 2$ and $n = \frac{1}{2}$. As a representative case of the above results consider $n = 2$, $\gamma = 7/5$. The straight streamlines in this example are $\theta = 0$ and $\theta = \pi/2$, and this corresponds to a compressible flow about a 90° corner. This particular choice of n is exceptional, in that one of the solutions of the hypergeometric equation (22) is a polynomial, and the other is an infinite series involving a logarithmic term.

The streamfunction in this case is taken to be

$$(37) \qquad \psi = P_2(\tau)\sin 2\theta = \left[K_2 \tau F^{(1)}\left(\tfrac{5}{2},-3,3;\tau\right) + \tau^{-1}F^{(2)}\left(\tfrac{1}{2},-5,-1;\tau\right)\right]\sin 2\theta,$$

where

$$F^{(1)}\left(\tfrac{5}{2},-3,3;\tau\right) = \frac{1}{32}(32 - 80\tau + 70\tau^2 - 21\tau^3),$$

$$F^{(2)}\left(\tfrac{1}{2},-5,-1;\tau\right) = 1 + \frac{5}{2}\tau - \frac{15}{2}\tau^2 F\left(\tfrac{5}{2},-3,3;\tau\right)\log\tau + \frac{120}{\Gamma(\frac{1}{2})}\sum_{\nu=3}^{\infty}\frac{\Gamma(\nu+\frac{1}{2})\Gamma(\nu-5)}{\Gamma(\nu-1)\nu!}\tau^\nu,$$

$$K_2 = -\left[\frac{d}{d\tau}(\tau^{-1}F^{(2)})/\frac{d}{d\tau}(\tau F^{(1)})\right]_{\tau=\frac{1}{6}} = 123.12.$$

The coordinate functions are, from (24),

$$(38)\qquad \begin{cases} x_2 = \tau^{-\frac{1}{2}}(1-\tau)^{-\beta}\left[\tfrac{1}{3}(\tau P_2' - P_2)\cos 3\theta + (\tau P_2' + P_2)\cos\theta\right] \\ y_2 = \tau^{-\frac{1}{2}}(1-\tau)^{-\beta}\left[\tfrac{1}{3}(\tau P_2' - P_2)\sin 3\theta - (\tau P_2' + P_2)\sin\theta\right] \end{cases}$$

and the sonic limit line in the physical plane is consequently the astroid

$$\begin{cases} x_2 = -\tfrac{1}{3}\left[\tau_t^{-\frac{1}{2}}(1-\tau_t)^{-\beta}P_2(\tau_t)\right](\cos 3\theta - 3\cos\theta), \\ y_2 = -\tfrac{1}{3}\left[\tau_t^{-\frac{1}{2}}(1-\tau_t)^{-\beta}P_2(\tau_t)\right](\sin 3\theta + 3\sin\theta), \end{cases}$$

or on eliminating θ

$$(x_2+y_2)^{\frac{2}{3}} + (x_2-y_2)^{\frac{2}{3}} = \left[4\sqrt{2}\,\tau_t^{-\frac{1}{2}}(1-\tau_t)^{-\beta}P_2(\tau_t)\right]^{\frac{2}{3}}.$$

The supersonic limit line in the hodograph is given by

$$(39)\qquad \tan 2\theta = \pm\frac{1}{\tau}\sqrt{\frac{6\tau-1}{1-\tau}}\cdot\frac{P_2}{P_2'},$$

and its image in the physical plane is obtained from (38).

The critical streamline is

$$\psi_c = P_2(\tau_t) = 22.586,$$

and the asymptotic streamline is*

$$\psi_a = P_2(1) = \kappa_2 F^{(1)}(\tfrac{5}{2},-3,3;1) + F^{(2)}(\tfrac{1}{2},-5,-1;1) = \kappa_2\,\frac{\Gamma(3)\Gamma(\frac{7}{2})}{\Gamma(\frac{1}{2})\Gamma(6)} + \frac{\Gamma(-1)\Gamma(\frac{7}{2})}{\Gamma(-\frac{3}{2})\Gamma(4)} = 4.2256.$$

---

*The expansion

$$F(a,b,c;\tau) = \frac{\Gamma(c)\Gamma(c-a-b)}{\Gamma(c-a)\Gamma(c-b)}F(a,b,1+a+b-c;1-\tau) + \frac{\Gamma(a+b-c)\Gamma(c)}{\Gamma(a)\Gamma(b)}(1-\tau)^{c-a-b}F(c-a,c-b,1+c-a-b;1-\tau)$$

is used near $\tau = 1$.

The streamline corresponding to any $\psi = \psi_0$ is obtained from (37) and (38).

Graphs of the limit lines and selected streamlines in the hodograph and in the physical plane, respectively, are presented in Figs. 9 and 10.** The manner in which the sheets corresponding to the physical plane must be connected is indicated diagrammatically in Fig. 11.

As another example of the foregoing, this time exhibiting a sonic limit line of the epicycloidal type (namely a nephroid), we select the case $n = \frac{1}{2}$. Here both solutions of the hypergeometric equation are regular and represented by infinite series:

$$(40)\qquad \psi(\tau,\theta) = P_{\frac{1}{2}}(\tau)\sin\frac{\theta}{2} = \left[K_{\frac{1}{2}}\tau^{\frac{1}{4}}F^{(1)}(a,b,\tfrac{3}{2};\tau) + \tau^{-\frac{1}{4}}F^{(2)}(a-\tfrac{1}{2},b-\tfrac{1}{2},\tfrac{1}{2};\tau)\right]\sin\frac{\theta}{2}$$

where

$$a,b = \tfrac{1}{4}(-4 \pm \sqrt{31}\,)\ ,$$

$$F^{(1)}(a,b,\tfrac{3}{2};\tau) = \frac{\Gamma(\frac{3}{2})}{\Gamma(a)\Gamma(b)}\sum_{\nu=0}^{\infty}\frac{\Gamma(\nu+a)\Gamma(\nu+b)}{\Gamma(\nu+\frac{3}{2})\nu!}\ ,$$

$$F^{(2)}(a-\tfrac{1}{2},b-\tfrac{1}{2},\tfrac{1}{2};\tau) = \frac{\Gamma(\frac{1}{2})}{\Gamma(a-\frac{1}{2})\Gamma(b-\frac{1}{2})}\sum_{\nu=0}^{\infty}\frac{\Gamma(\nu+a-\frac{1}{2})\Gamma(\nu+b-\frac{1}{2})}{\Gamma(\nu+\frac{1}{2})\nu!}\tau^{2}$$

$$K_{\frac{1}{2}} = -\left[\frac{d}{d\tau}(\tau^{-\frac{1}{4}}F^{(2)}) \,/\, \frac{d}{d\tau}(\tau^{\frac{1}{4}}F^{(1)})\right]_{\tau=\frac{1}{6}} = 3.42054.$$

The mapping to the physical plane is given by

$$(41)\qquad \begin{cases} x_{\frac{1}{2}} = \tau^{-\frac{1}{2}}(1-\tau)^{-\frac{5}{2}}\left[-\frac{1}{3}(2\tau P'_{\frac{1}{2}} - \frac{1}{2}P_{\frac{1}{2}})\cos\frac{3}{2}\theta + (2\tau P'_{\frac{1}{2}} + \frac{1}{2}P_{\frac{1}{2}})\cos\frac{1}{2}\theta\right] \\ y_{\frac{1}{2}} = \tau^{-\frac{1}{2}}(1-\tau)^{-\frac{5}{2}}\left[-\frac{1}{3}(2\tau P'_{\frac{1}{2}} - \frac{1}{2}P_{\frac{1}{2}})\sin\frac{3}{2}\theta + (2\tau P'_{\frac{1}{2}} + \frac{1}{2}P_{\frac{1}{2}})\sin\frac{1}{2}\theta\right] \end{cases}$$

**In the actual computation of these flows use was made of the tables in [4] and [8], taking due account of the errors in [8] which were pointed out in [14].

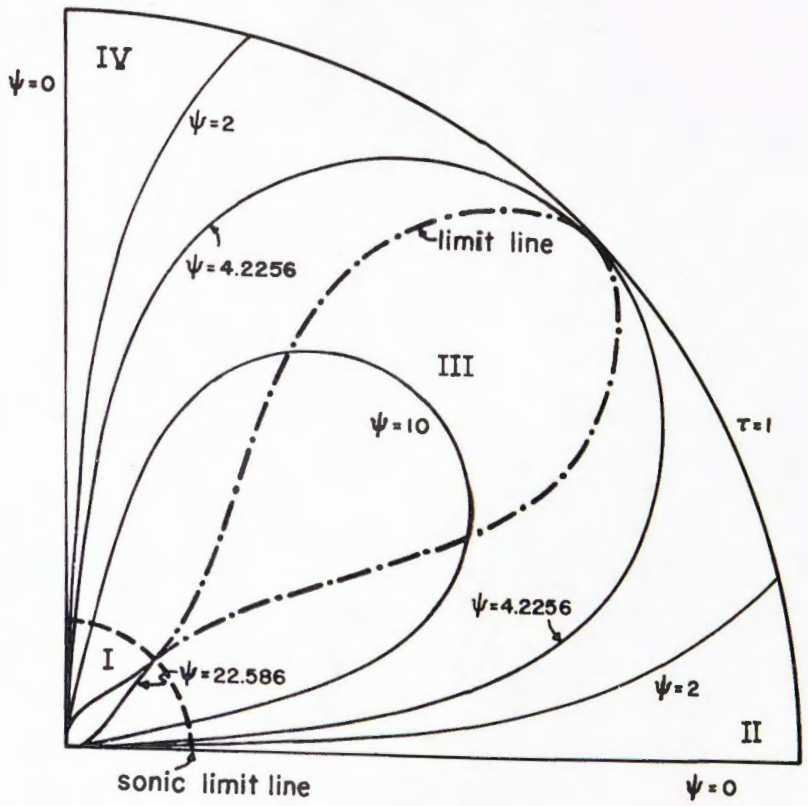

Fig. 9: Case n=2. Hodograph plane

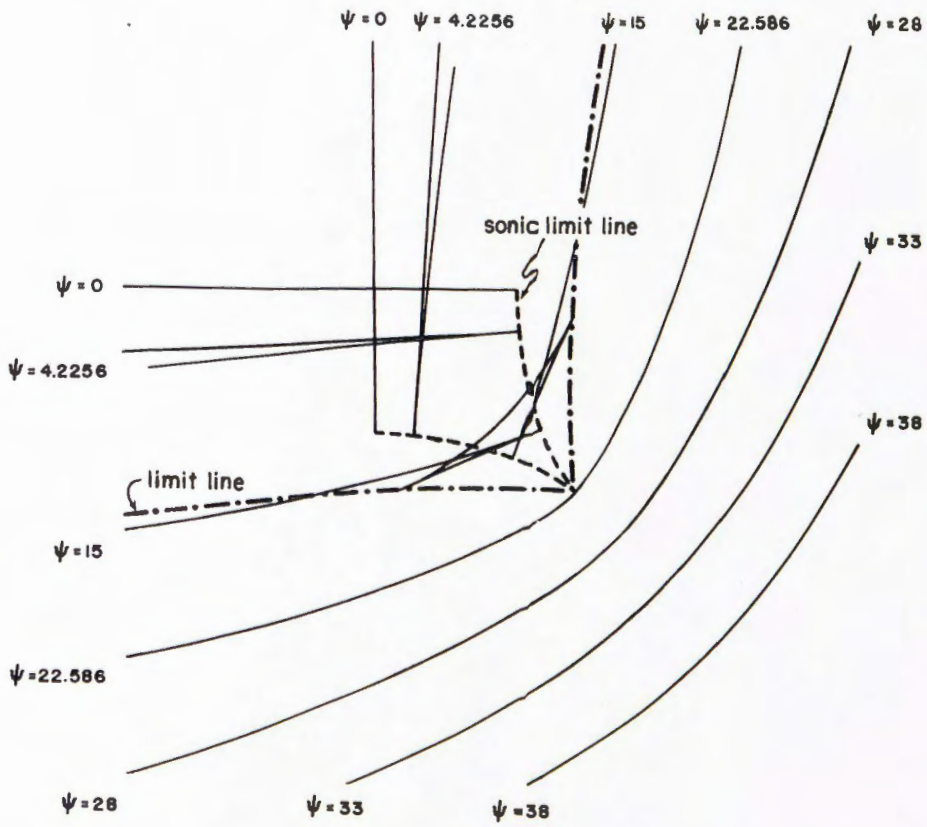

Fig. 10: Case n=2. Physical plane

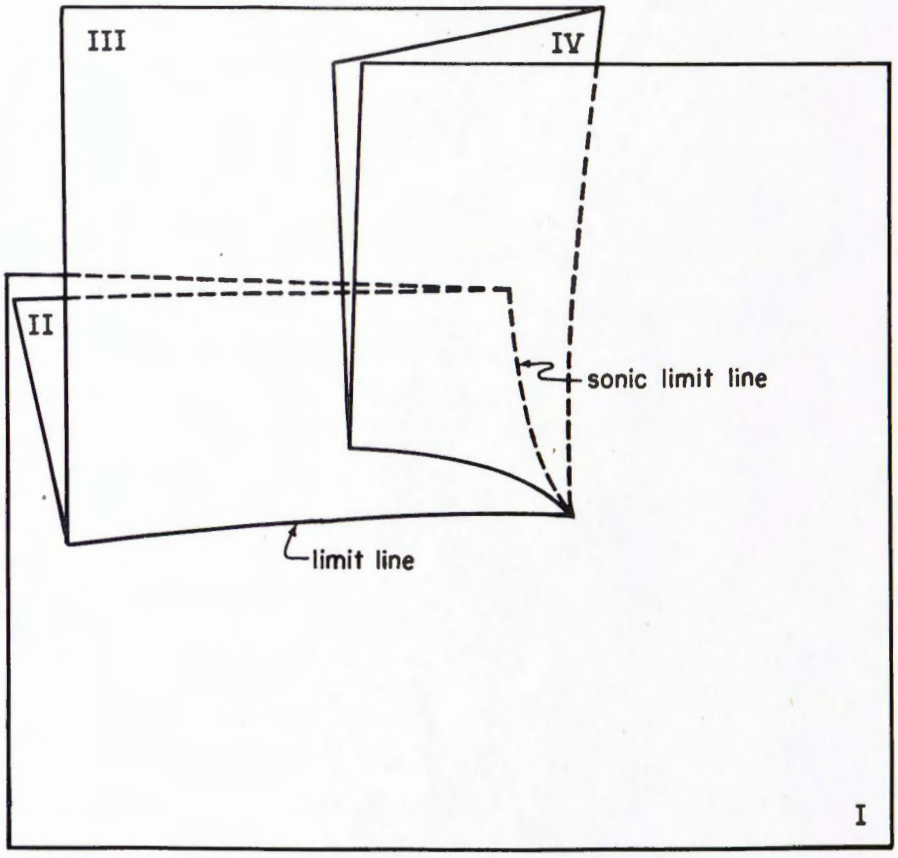

Fig 11: Case n=2. Sketch of multi-sheeted surface corresponding to physical plane

and the sonic limit line is the nephroid

$$\begin{cases} x_{\frac{1}{2}} = \frac{1}{2}\,\tau_t^{-\frac{1}{2}}(1-\tau_t)^{-\frac{5}{2}}P_{\frac{1}{2}}(\tau_t)\left(\frac{1}{3}\cos\tfrac{3}{2}\theta + \cos\tfrac{1}{2}\theta\right) \\ y_{\frac{1}{2}} = \frac{1}{2}\,\tau_t^{-\frac{1}{2}}(1-\tau_t)^{-\frac{5}{2}}P_{\frac{1}{2}}(\tau_t)\left(\frac{1}{3}\sin\tfrac{3}{2}\theta + \sin\tfrac{1}{2}\theta\right). \end{cases}$$

The supersonic limit line in the physical plane is obtained from (41) and

$$\tan\tfrac{1}{2}\theta = \pm\frac{1}{4\tau}\sqrt{\frac{6\tau-1}{1-\tau}}\cdot\frac{P_{\frac{1}{2}}}{P'_{\frac{1}{2}}}. \tag{42}$$

The critical streamline is

$$\psi_c = P_{\frac{1}{2}}(\tau_t) = 3.68576,$$

and the asymptotic streamline is

$$\psi_a = P_{\frac{1}{2}}(1) = K_{\frac{1}{2}}F(a,b,\tfrac{3}{2};1) + F(a-\tfrac{1}{2},b-\tfrac{1}{2},\tfrac{1}{2};1)$$

$$= K_{\frac{1}{2}}\,\frac{\Gamma(\frac{3}{2})\Gamma(\frac{3}{2}-a-b)}{\Gamma(\frac{3}{2}-a)\Gamma(\frac{3}{2}-b)} + \frac{\Gamma(\frac{1}{2})\Gamma(\frac{3}{2}-a-b)}{\Gamma(1-a)\Gamma(1-b)} = 3.37976.$$

The streamlines in the physical plane are obtained from (40) and (41).

Graphs of the limit lines and selected streamlines in the hodograph and physical plane for this case are shown in Figs. 12 and 13. Fig. 14 is a diagrammatic representation of the sheeted surface replacing the physical plane.

An interesting feature of this flow is that sheet I overlaps with itself.

X. <u>The sonic limit line flow for n = 1</u>. The case n = 1 is exceptional in that both solutions of the form (19) and (20) can be given in closed form, in fact

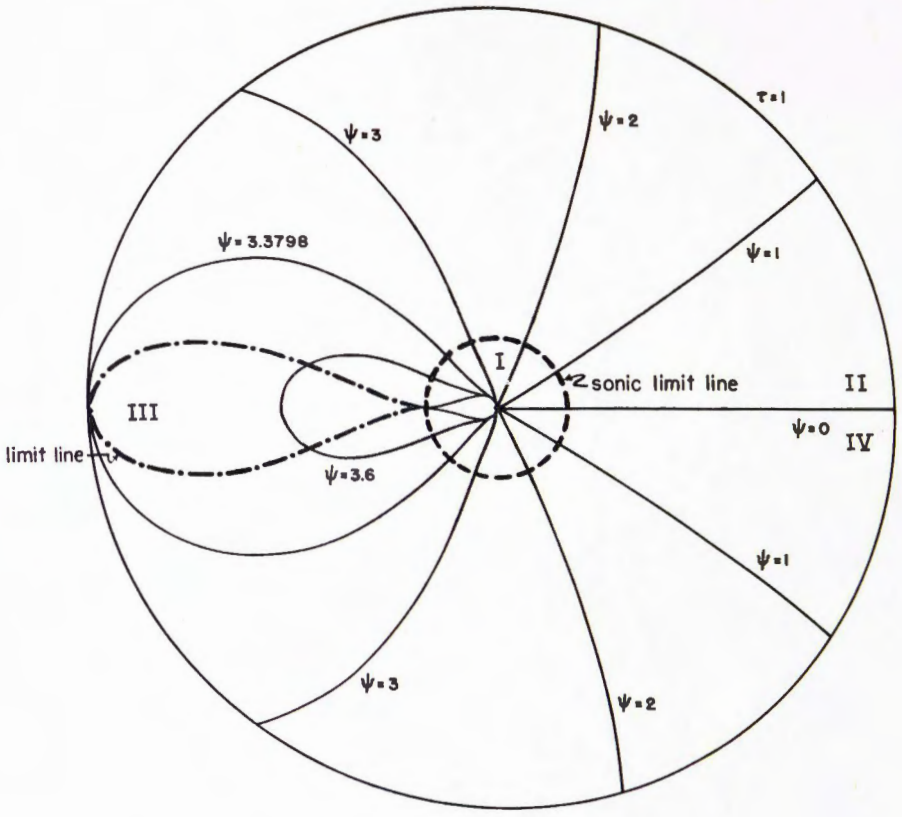

Fig. 12: Case n=½. Hodograph plane

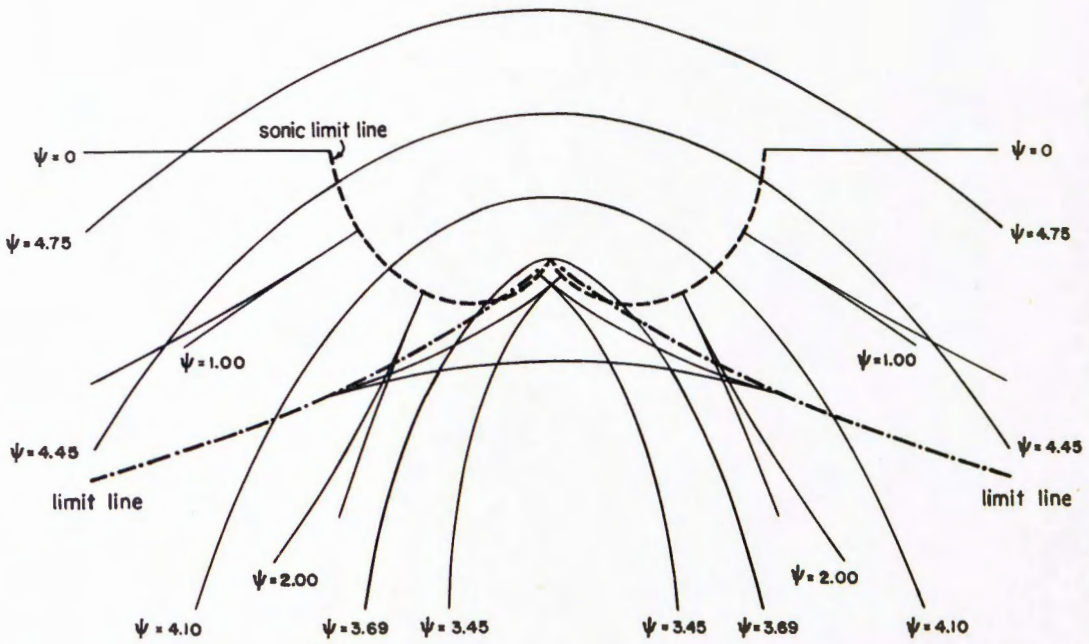

Fig13: Case n=½. Physical plane

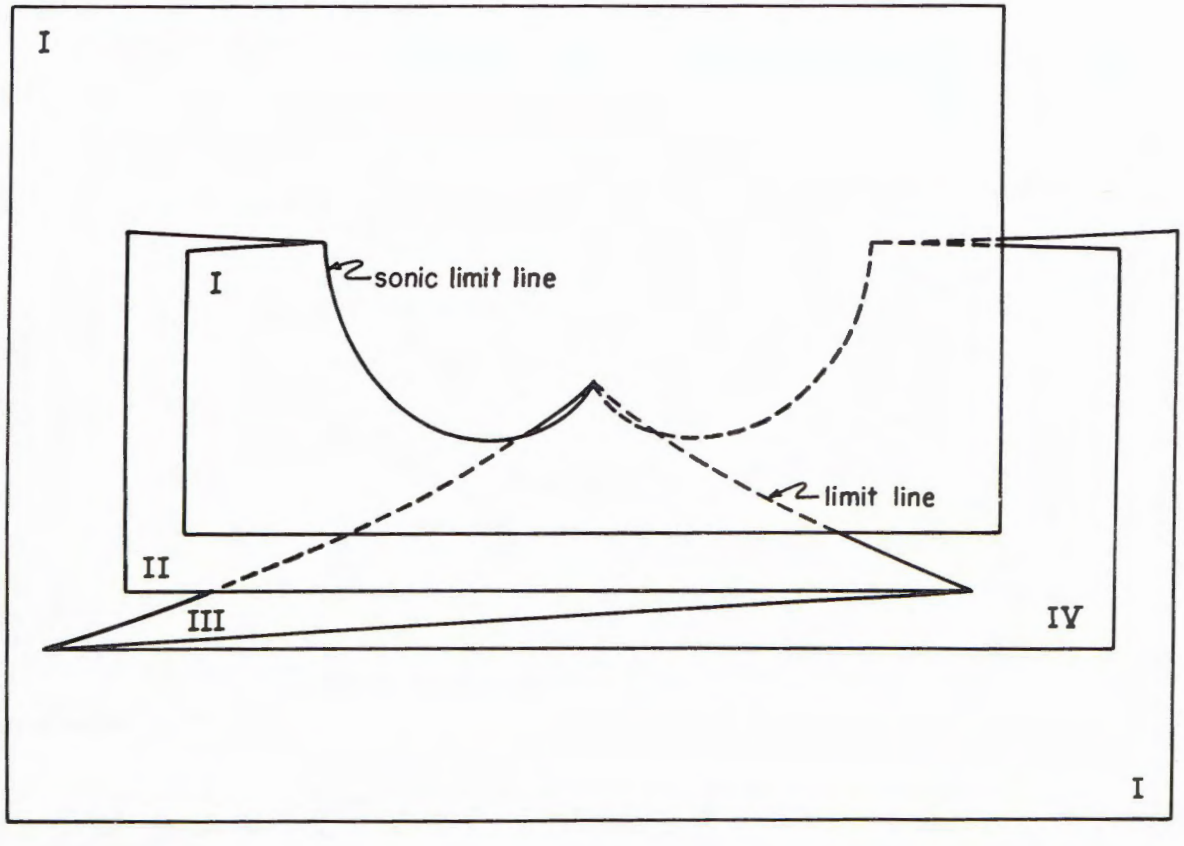

Fig.14: Case n=½. Sketch of multi-sheeted surface corresponding to physical plane

$$F_1^{(1)}(\tau) = F(1,-\beta,2;\tau) = \frac{1}{(1+\beta)\tau}\left[1 - (1-\tau)^{\beta+1}\right]$$

$$F_1^{(2)}(\tau) = \lim_{n\to 1} F(a_n-n, b_n-n, 1-n;\tau) = 1 + \tfrac{1}{2}\frac{1}{\beta+1}\left[1 - (1-\tau)^{\beta+1}\right].$$

Since the combination $H_1(\tau)$ will contain a linear combination of the basic functions τ^{-1} and $\tau^{-1}(1-\tau)^{\beta+1}$ we may write the streamfunction for this case in the form

$$\psi(\tau,\theta) = P_1(\tau)\sin\theta = \tau^{-\frac{1}{2}}\left[\kappa + (1-\tau)^{\beta+1}\right]\sin\theta \tag{43}$$

where in order to satisfy (23) we must take

$$\kappa = -2\left(\frac{2\beta}{2\beta+1}\right)^{\beta} = -2\left(\frac{\sqrt{30}}{6}\right)^{5} = -1.2679.$$

In the limit of the incompressible case this solution gives rise to the flow around a semi-infinite plane barrier, $\theta = 0$, $r \geq 0$, the streamlines being confocal parabolas.

The transformation to the physical plane is given from (25) by

$$\begin{cases} 2x_1 = [\kappa\tau^{-1}(1-\tau)^{-\beta} + \beta + \tau^{-1}]\cos 2\theta + \kappa\beta\int\tau^{-1}(1-\tau)^{-\beta-1}d\tau + (2\beta+1)\log\tau \\ 2y_1 = [\kappa\tau^{-1}(1-\tau)^{-\beta} + \beta + \tau^{-1}]\sin 2\theta - (\beta+1)(2\theta) \end{cases} \tag{44}$$

where the integral in the first expression of (44) can be evaluated in closed form for $\beta = \frac{5}{2}$ $(\gamma = \frac{7}{5})$ and is in fact

$$\int\tau^{-1}(1-\tau)^{-\beta-1}d\tau = \log\frac{1-\sqrt{1-\tau}}{1+\sqrt{1+\tau}} + \frac{2}{5}\frac{1}{(1-\tau)^{\frac{5}{2}}} + \frac{2}{3}\frac{1}{(1-\tau)^{\frac{3}{2}}} + 2\frac{1}{(1-\tau)^{\frac{1}{2}}} \tag{45}$$

and the sonic limit line in the physical plane is consequently the cycloid

$$(46) \qquad \begin{cases} 2x_1 = (\beta+1)\cos 2\theta + \text{constant} \\ 2y_1 = (\beta+1)\sin 2\theta - (\beta+1)(2\theta). \end{cases}$$

The supersonic limit line in the hodograph is given by

$$(47) \qquad \tan\theta = \pm \left[\frac{(2\beta+1)\tau - 1}{1-\tau}\right]^{\frac{1}{2}} \left\{\frac{\kappa + (1-\tau)^{\beta+1}}{\kappa + [1+(1+2\beta)\tau](1-\tau)^{\beta}}\right\}.$$

The critical streamline is from (43)

$$\psi_c = P_1(\tau_t) = -2\frac{\beta+1}{\sqrt{2\beta+1}}\left(\frac{2\beta}{2\beta+1}\right)^{\beta} = -\frac{175\sqrt{5}}{216} = -1.8116$$

and the asymptotic streamline is

$$\psi_a = P_1(1) = \kappa = -1.2679.$$

The streamlines and the supersonic limit line in the physical plane are obtained from (43) and (44), and (47) and (44), respectively.

A graph of the critical curves in the hodograph plane as well as selected streamlines is presented in Fig. 15. A sketch of the corresponding curves in the physical plane is shown in Fig. 16. The way in which the sheets are connected is shown diagrammatically in Fig. 17.

XI. Superposition of sonic limit line flows for different n. The isolated sonic limit line. Superposition of a finite number of sonic limit line solutions (18) for different n will again yield a flow with a sonic limit line. The coordinate functions may be found by adding the coordinate functions (24)

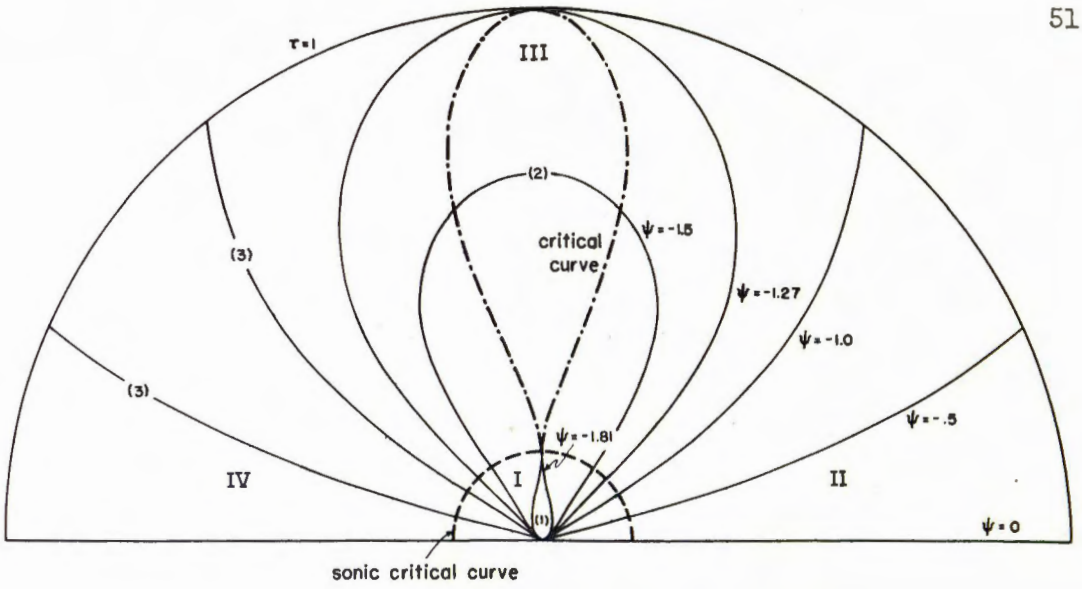

Fig.15 Hodograph plane Case n=1.

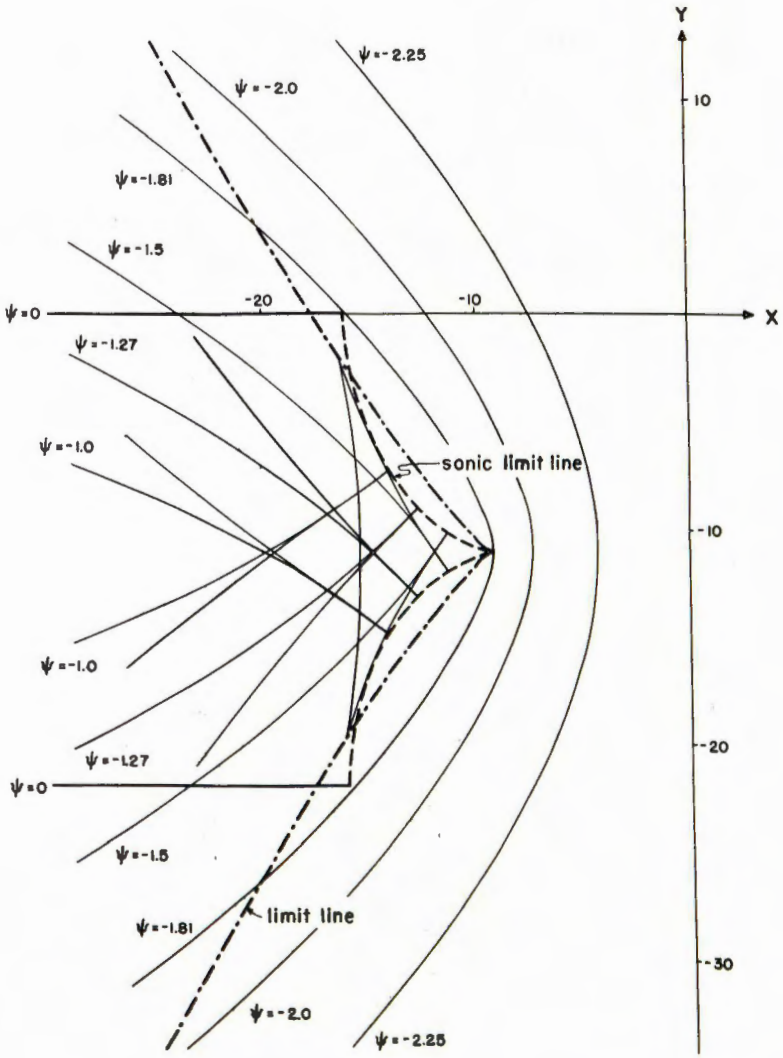

Fig.16 Physical plane Case n=1.

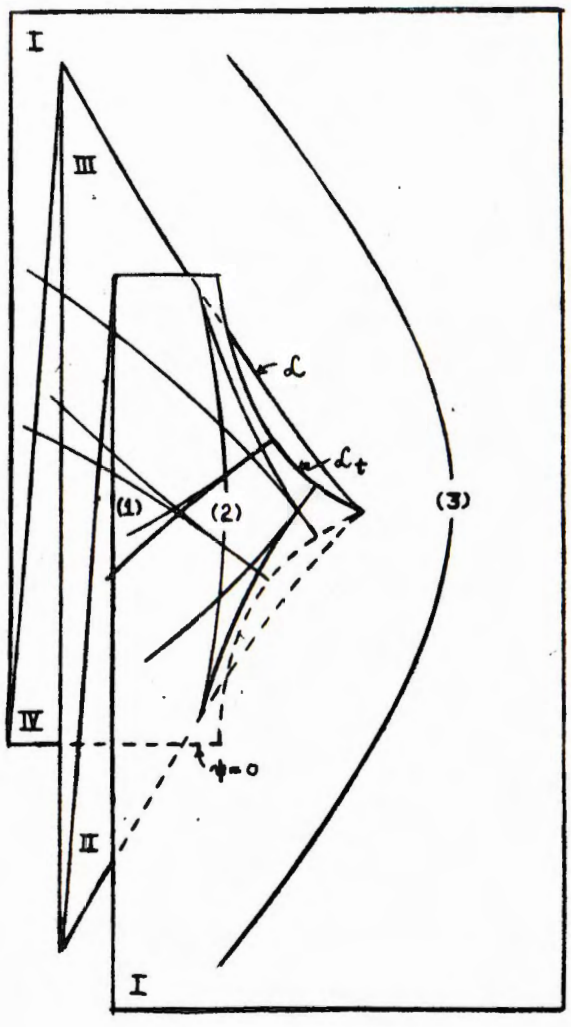

Fig.17: Sketch of multi-sheeted surface corresponding to physical plane. Case n=1.

of the individual sonic limit line flows. Unfortunately the simple geometric character of the sonic limit line in the physical plane for the separate solutions is thereby destroyed.

However, a simple rule for the geometrical construction of the sonic limit line in the physical plane may still be given. Draw the sonic limit lines which correspond to the individual solutions. Then add the coordinates of the points on the individual sonic limit lines at which the slopes of the latter are the same. The curve constructed in this manner will be the sonic limit line of the combined solution. This follows from the fact that a sonic limit line is always perpendicular to the streamline, so that one is in fact adding for the same value of θ, i.e. for the same point in the hodograph.

In section VI we noted that for any n, the flow constructed from (18) necessarily contained a supersonic limit line in addition to the sonic limit line. The question arises whether, by superposition, a flow can be constructed which is devoid of any supersonic limit singularities and contains only a sonic limit line.

Now given the sonic limit line solution (18) for any n, we can, by adding to it a suitable radial flow solution ($n = 0$), obtain a flow such that (i) the resulting flow continues to possess a sonic limit line and (ii) χ_θ retains the same sign along the sonic line. Hence the sonic line consists entirely of ordinary limit points ($\chi_\theta \neq 0$) and it must therefore be an isolated sonic limit line by Theorem 8. In fact we shall see that even in the limiting case of the above construction, when χ_θ is allowed to take zero values (without changing sign: $\chi_{\theta\theta} = 0$, cf. Theorem 14), the flow still has an isolated sonic limit line (see section IV(ii); an example will be presented in Sec. XII).

For any n, we have for the solution (18)

$$\psi_\theta(\tau_t,\theta) = P_n(\tau_t)\ n\cos n\theta\ ,$$

whereas for the radial flow, whose streamfunction is

(48) $$\psi(\tau,\theta) = k\theta,$$

we have

$$\psi_\theta(\tau_t,\theta) = k.$$

If we add (18) and (48) and require that ψ_θ does not change sign anywhere on $\tau = \tau_t$ we must choose k such that

(49) $$|k| \geq \mp nP_n(\tau_t) \quad \text{according as} \quad P_n(\tau_t) \lesseqgtr 0.$$

Clearly the addition of the radial flow does not affect the vanishing of ψ_τ on the sonic line; hence the resulting flow will continue to possess a sonic limit line. Moreover if the strict inequality holds in (49) we have $\psi_\theta \neq 0$ for $\tau = \tau_t$ and by Theorem 8 the sonic limit line is isolated.

What happens to the supersonic limit line which appears in a flow corresponding to (18) when the radial solution is added to it? From the streamfunction of the combined flow

$$\psi(\tau,\theta) = k\theta + P_n(\tau)\sin n\theta$$

we see that the supersonic limit line is given by

(50) $$k + P_n n\cos n\theta \pm \sqrt{PQ}\ P_n' \sin n\theta = 0,$$

where we have used the abbreviation

(51) $$P = \frac{2\tau(1-\tau)^{\beta+1}}{(2\beta+1)\tau - 1}\ , \qquad Q = \frac{2\tau}{(1-\tau)^\beta}\ .$$

Equation (50) may be written

$$\cos\left[n\theta \mp \delta(\tau)\right] = \frac{k}{\sqrt{n^2 P_n^2 + PQP_n'^2}} \,,$$

hence for given k, only those values of τ for which

$$\Delta = n^2 P_n^2 + PQP_n'^2 - k^2 > 0 \tag{52}$$

will give real values of θ.

Let us investigate the region in the k,τ-plane for which this inequality is satisfied for some fixed value of n. Certainly the region is bounded by the lines $\tau = \tau_t$ and $\tau = 1$. Differentiating $k^2 = n^2 P_n^2 + PQP_n'^2$ with respect to τ, making use of Chaplygin's equation in the form $PQP_n'' + PQ'P_n' + n^2 P_n = 0$ (cf. (9)), and (51) we have

$$\frac{d(k^2)}{d\tau} = \frac{d}{d\tau}(n^2 P_n^2 + PQP_n'^2) = P_n'^2(P'Q - PQ') = -\frac{8\beta(2\beta+1)\tau^3}{\left[(2\beta+1)\tau - 1\right]^2} P_n'^2 < 0 \text{ for } \tau_t < \tau < 1,$$

so that the boundary curve $k^2 = n^2 P_n^2 + PQP_n'^2$ of the region (52) is monotonically decreasing with increasing τ in the range $\tau_t < \tau < 1$. A sketch of the region (52) is presented in Fig. 18.

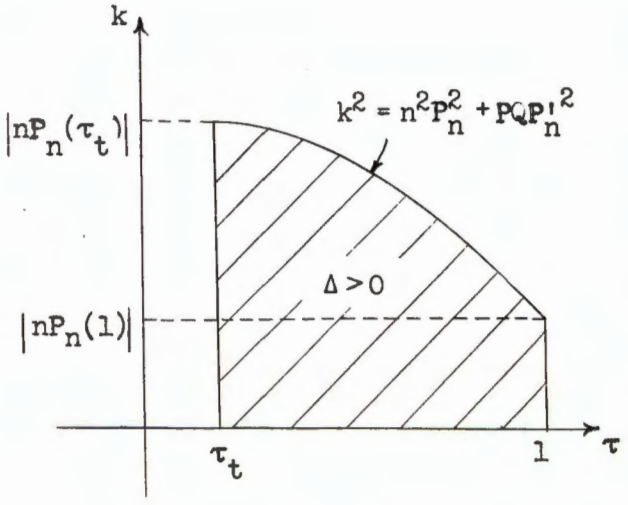

Fig. 18

From this graph we may interpret the extent of the supersonic limit line in the hodograph. Clearly for $k = 0$ (the pure sonic limit line flow) the supersonic limit line extends from $\tau = \tau_t$ to $\tau = 1$. This remains true for values of k up to $k = |nP_n(1)|$. However as k increases from $|nP_n(1)|$ to $|nP_n(\tau_t)|$ the supersonic limit line detaches from the maximum

circle $\tau = 1$ (while remaining attached to the sonic circle $\tau = \tau_t$ since $\psi_\theta = 0$ at some points there) and shrinks towards the sonic circle. For values of k such that $|nP_n(1)| < k < |nP_n(\tau_t)|$ the supersonic limit line thus extends only up to a circle of radius τ_m, say, and $\tau_m \to \tau_t$ as $k \to |nP_n(\tau_t)|$. For $|nP_n(\tau_t)| < k$ no real branches of the supersonic limit line exist.

XII. A flow with isolated sonic limit line. As a simple example of a flow with an isolated sonic limit line (see Sec. XI) we superpose the sonic limit line flow for $n = 1$ and the radial flow corresponding to $n = 0$, i.e.

$$\psi = k\theta + \tau^{-\frac{1}{2}}\left[\kappa + (1-\tau)^{\beta+1}\right]\sin\theta,$$

where as in (43)

$$\kappa = -2\left(\frac{2\beta}{2\beta+1}\right)^{\beta} \qquad (= -1.267876 \text{ for } \gamma = \tfrac{7}{5}),$$

and since $P_1(\tau_t) = -2\,\frac{(\beta+1)}{\sqrt{2\beta+1}}\left(\frac{2\beta}{2\beta+1}\right)^{\beta} < 0$, k must be chosen such that

$$|k| \geq -P_1(\tau_t) = 2\,\frac{(\beta+1)}{\sqrt{2\beta+1}}\left(\frac{2\beta}{2\beta+1}\right)^{\beta},$$

see (49). In view of our earlier study of higher-order sonic limit singularities [section IV(ii)] and the preceding section, we choose k to be exactly

$$k = 2\,\frac{(\beta+1)}{\sqrt{2\beta+1}}\left(\frac{2\beta}{2\beta+1}\right)^{\beta} \qquad (= 1.811629 \text{ for } \gamma = \tfrac{7}{5}),$$

since then

$$\psi_\theta = k + \tau^{-\frac{1}{2}}\left[\kappa + (1-\tau)^{\beta+1}\right]\cos\theta,$$

$$\psi_{\theta\theta} = -\tau^{-\frac{1}{2}}\left[\kappa + (1-\tau)^{\beta+1}\right]\sin\theta,$$

and the point $\tau = \tau_t$, $\theta = 0$ will be a higher-order sonic limit point on a sonic limit line where $\psi_{\theta\theta} = 0$.

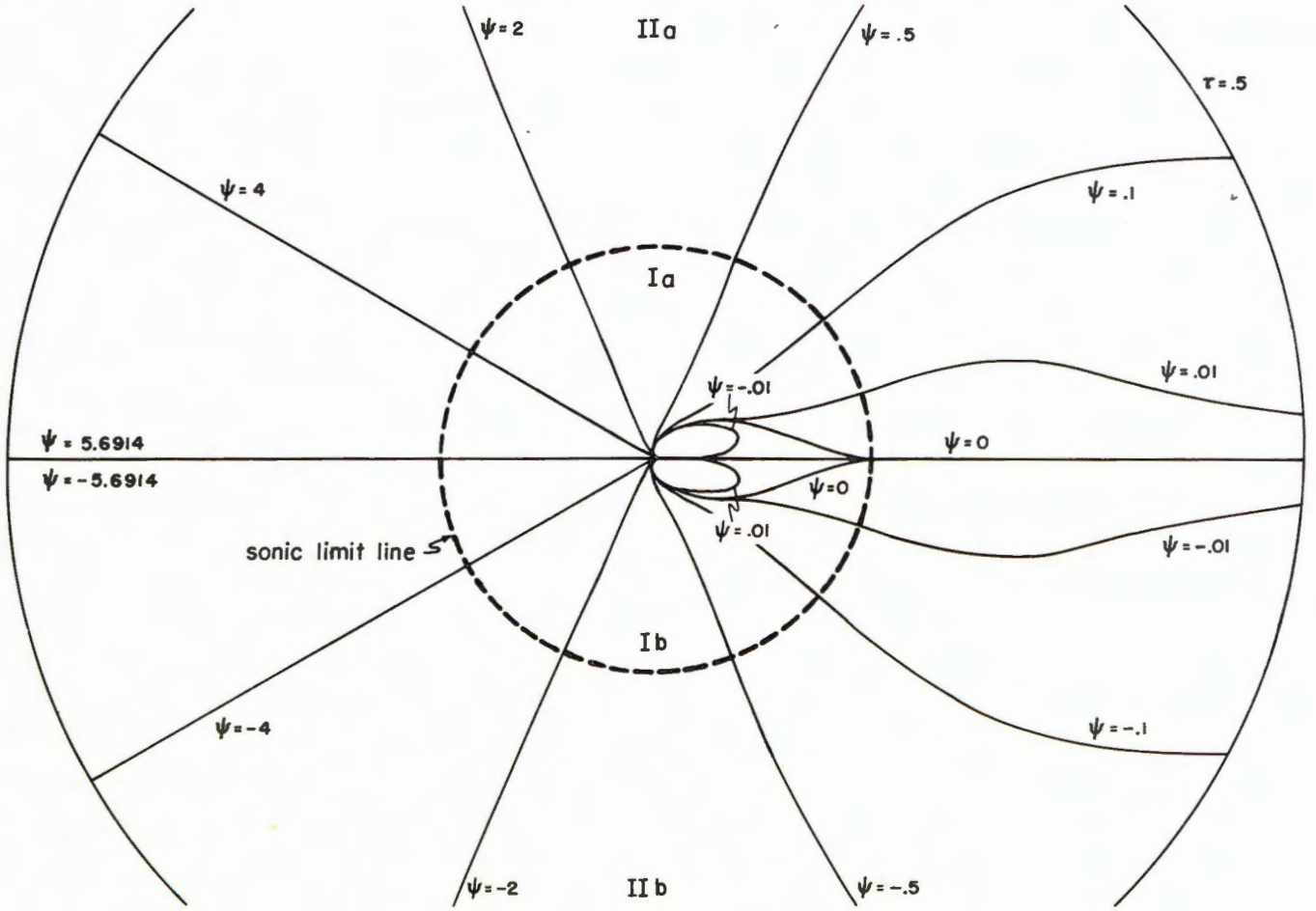

Fig. 19: Isolated sonic limit line. Hodograph plane

The coordinates in the physical plane are given by (cf. (44))

$$\begin{cases} 2x = [\kappa\tau^{-1}(1-\tau)^{-\beta} + \beta + \tau^{-1}]\cos 2\theta + \kappa\beta\int\tau^{-1}(1-\tau)^{-\beta-1}d\tau + (2\beta+1)\log\tau \\ \qquad\qquad + 2k\tau^{-\frac{1}{2}}(1-\tau)^{-\beta}\cos\theta, \\ 2y = [\kappa\tau^{-1}(1-\tau)^{-\beta} + \beta + \tau^{-1}]\sin 2\theta - (\beta+1)(2\theta) + 2k\tau^{-\frac{1}{2}}(1-\tau)^{-\beta}\sin\theta, \end{cases}$$

where the integral in the first expression can be evaluated in closed form (45) for $\gamma = 7/5$. The sonic limit line in the physical plane is then given by

$$\begin{cases} 2x = 2(\beta+1)\cos\theta[2 - \cos\theta] + (\beta+1) + \kappa\beta\int_{\frac{1}{2\beta+1}}^{1}\tau^{-1}(1-\tau)^{-\beta-1}d\tau + (2\beta+1)\log\frac{1}{2\beta+1}, \\ 2y = 2(\beta+1)\sin\theta[2 - \cos\theta] - 2(\beta+1)\theta. \end{cases}$$

This curve is the locus of a point moving harmonically on the extended diameter of a circle, while the circle in turn rolls on a straight line. It is a trochoid-like curve and does not possess any cusps.

The flow in the hodograph plane, and hence naturally also in the physical plane, is of quite a different character from that of the sonic limit line flows discussed previously.

In the hodograph plane the streamlines no longer form lemniscate-like loops inside a circular sector, but behave as shown in Fig. 19. For a given value of $\psi = \psi_0 > 0$, the streamline in the hodograph consists of two portions: (i) one above the horizontal axis which meets the sonic limit line and ranges from $\tau = 0$ through all subsonic and all supersonic values of τ to the maximum value $\tau = 1$, and (ii) one below the horizontal axis which starts at $\tau = 0$ and loops around back to $\tau = 0$ without attaining supersonic speeds. The two portions which make up the corresponding streamline $\psi = -\psi_0 < 0$ form the symmetric image of $\psi = \psi_0$ in the axis $\theta = 0$. This explains the symmetry of the figure. The streamline $\psi = 0$ falls into the above pattern

in a limiting sense (see Fig. 20); it degenerates into the straight segment $\theta = 0$ plus the symmetric cusped curve which passes through the higher-order limit point $\tau = \tau_t$, $\theta = 0$.

The corresponding streamlines in the physical plane therefore consist of subsonic-supersonic portions which are cusped at the sonic limit line, and regular, purely subsonic portions.

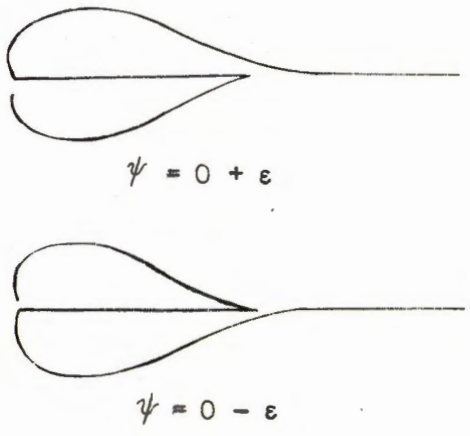

Fig. 20

To simplify the discussion of the streamlines in the physical plane we restrict ourselves first to that portion of the physical plane which corresponds to the upper half ($0 \leq \theta \leq \pi$) of the hodograph plane. In this range lie the cusped portions of some streamlines ($0 \leq \psi$) and the regular portions of the rest. Thus we expect the streamlines in the physical plane corresponding to this half of the hodograph to lie on two sheets (a subsonic and a supersonic sheet) and the others to lie partially on both sheets. From this and the variations of θ along the streamlines in the hodograph we thus infer the following picture (Fig. 21a). Note that parts of the subsonic sheets overlap in a manner similar to that in the second example of Sec. IX. By symmetry the portion of the sheeted surface corresponding to the lower half of the hodograph is as shown in Fig. 21b.

To obtain the complete picture we must join the two parts depicted in Figs. 21a and 21b along the line of symmetry PQR; the result is Fig. 22. Note that the entire surface consists of only two sheets - a subsonic and a supersonic sheet. However, the individual sheets overlap in parts, so that

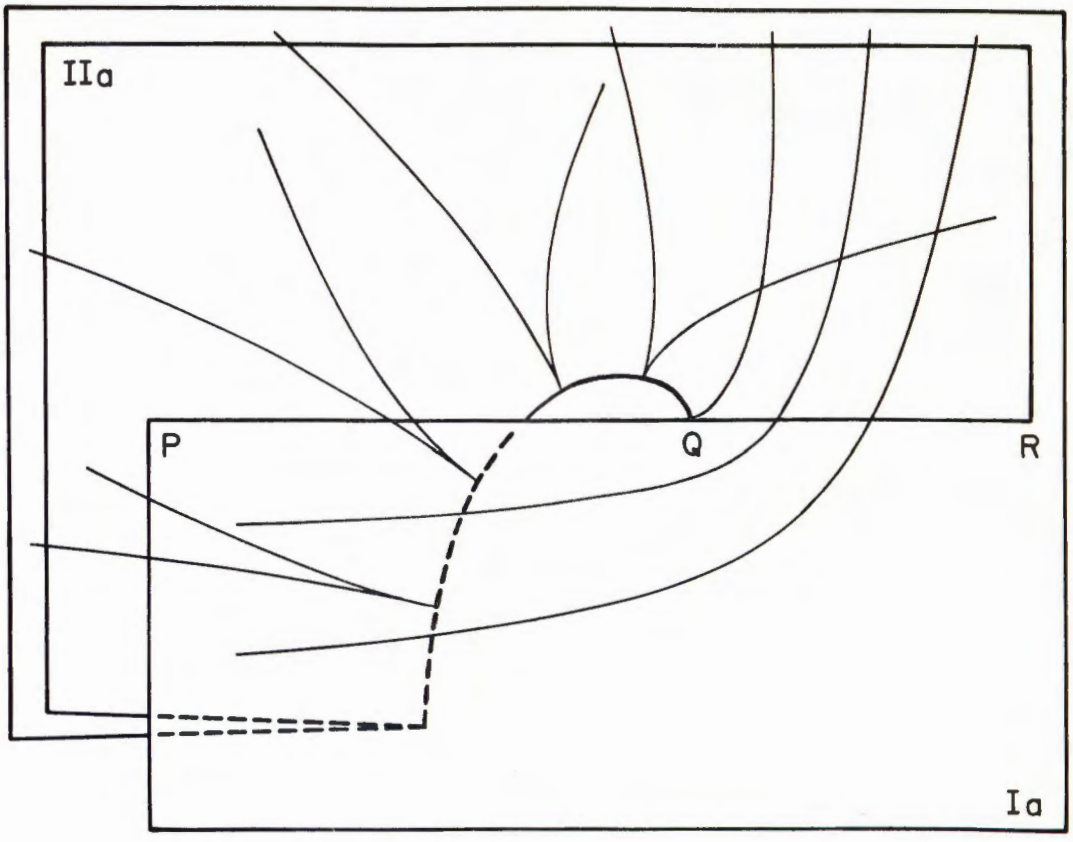

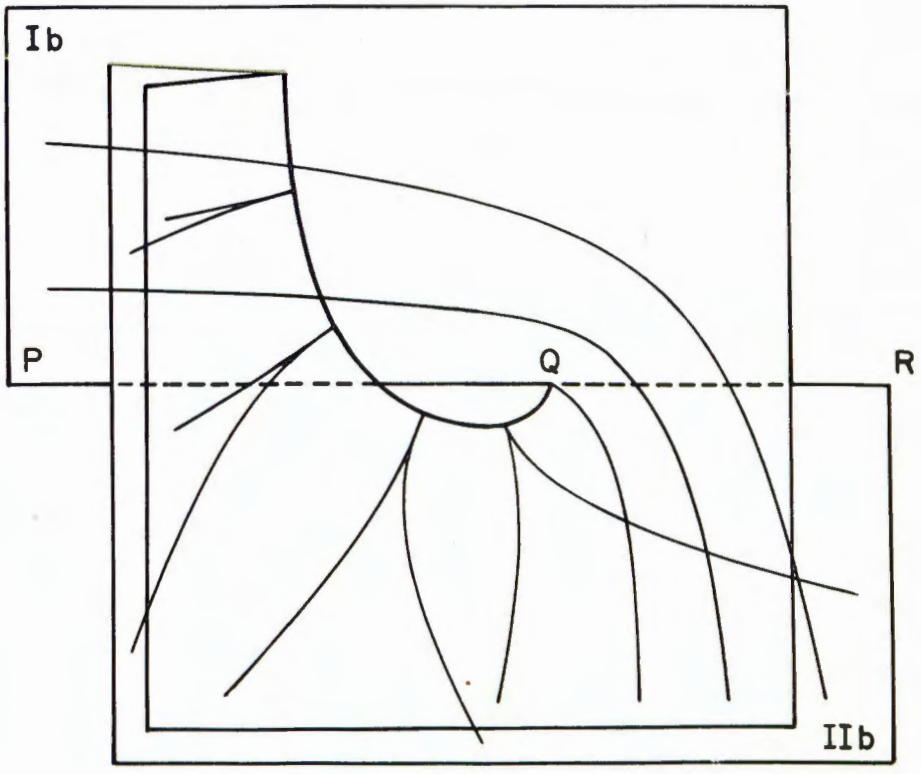

Figs. 21 a,b: Isolated sonic limit line. Physical plane (schematic).

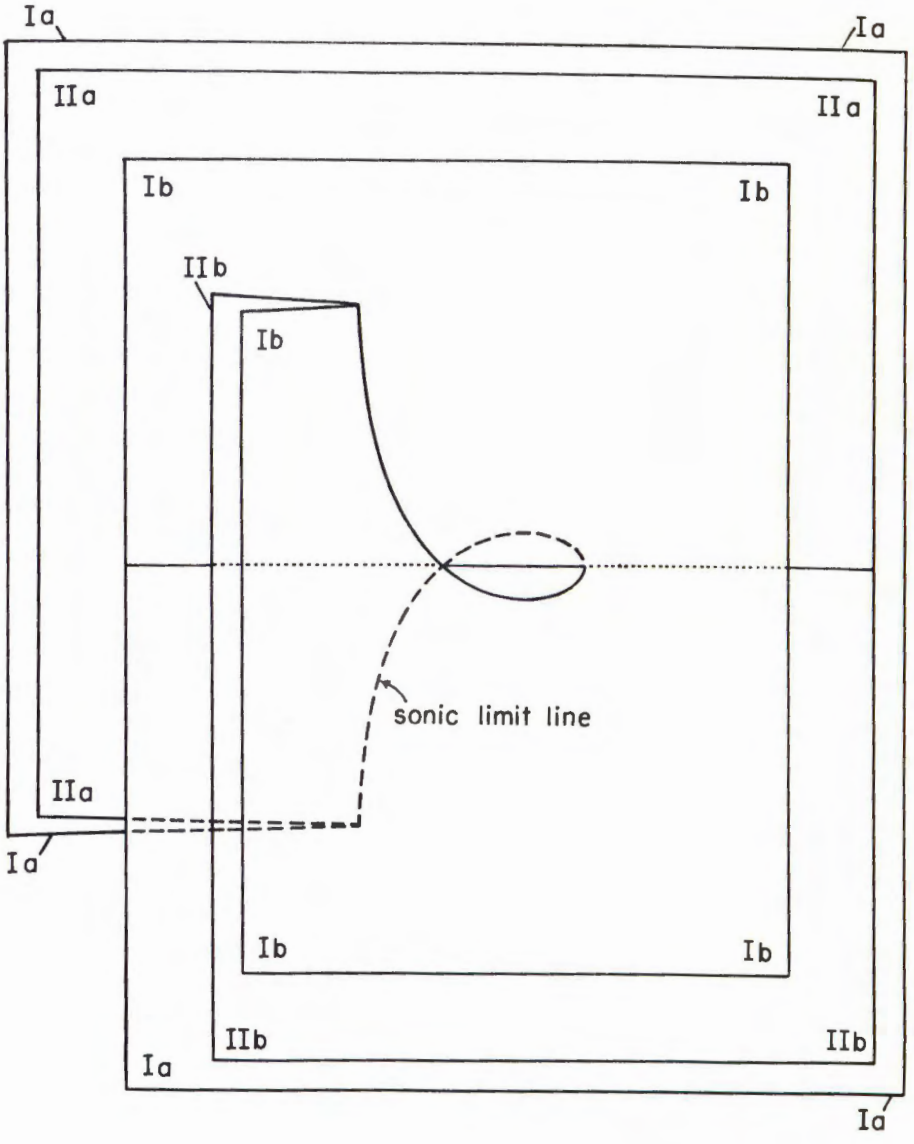

Fig. 22: Isolated sonic limit line. Sketch of multi-sheeted surface corresponding to physical plane.

there are regions of single-, triple-, and quintuple-valuedness in parts of the x,y-plane. The sonic limit line along which the sheets join is nowhere cusped.

APPENDIX

Asymptotic expansion of the sonic limit line solution. In order to construct sonic limit line flows by superimposing an infinite number of streamfunctions of the form (18) it is mandatory to know the behavior of $P_n(\tau)$ for large values of n, particularly in the neighborhood of the sonic value $\tau = \tau_t$. In this appendix we derive the asymptotic sonic limit line solution which holds in a one-sided neighborhood $\tau_t < \tau < \tau_1$, where τ_1 is some arbitrary point in the supersonic region.

As noted in Sec. VII the sonic limit line combination of hypergeometric functions

$$P_n(\tau) = K_n \tau^{\frac{n}{2}} F_n^{(1)}(\tau) + \tau^{-\frac{n}{2}} F_n^{(2)}(\tau) \tag{53}$$

satisfies the second-order ordinary differential equation

$$\frac{d^2P_n}{d\tau^2} + \frac{1-(1+\beta)\tau}{\tau(1-\tau)} \frac{dP_n}{d\tau} - n^2 \frac{1-(2\beta+1)\tau}{4\tau^2(1-\tau)} P_n = 0$$

which, on making the substitution

$$P_n(\tau) = z(\tau)\exp\left[-\tfrac{1}{2}\int \frac{1-(1+\beta)\tau}{\tau(1-\tau)}\, d\tau\right] = \frac{z(\tau)}{\sqrt{2\tau}(1-\tau)^{\beta/2}}$$

reduces to

$$\frac{d^2z}{d\tau^2} - \left[n^2 \frac{1-(2\beta+1)\tau}{4\tau^2(1-\tau)} - \frac{1-(2\beta+1)\tau}{4\tau^2(1-\tau)} + \frac{2+\beta}{4(1-\tau)^2}\right] z = 0. \tag{54}$$

This equation is of the general type

$$\frac{d^2z}{d\tau^2} - [n^2 q(\tau) + \chi(\tau)]\, z = 0$$

where $q(\tau)$ has a simple zero at $\tau = \tau_t$

$$q(\tau) \begin{cases} > 0 & 0 < \tau < \tau_t \\ = 0 & \tau = \tau_t \\ < 0 & \tau_t < \tau < 1 \end{cases}$$

and $\chi(\tau)$ is analytic in the interval $0 < \tau < 1$. For large n this equation has solutions which are monotonic for subsonic values of the argument τ and oscillatory for supersonic values (Stokes' phenomenon). A general method for finding asymptotic solutions of this type of equation in a neighborhood of the transition point was developed by R. E. Langer [9].

Briefly, Langer's result pertinent to our case is the following. The equation (54) has the asymptotic integrals

$$z_n^{(j)}(\tau) = V(\tau) X^{\frac{1}{3}} H_{\frac{1}{3}}^{(j)}(X) \qquad j=1,2. \tag{55}$$

where $H_{\frac{1}{3}}^{(j)}(X)$ represent the one-third order Hankel functions of j-th kind, and

$$U(\tau) = \int_{\tau_t}^{\tau} \sqrt{-q(\tau)}\, d\tau = -\arctan\sqrt{\frac{(2\beta+1)\tau-1}{1-\tau}} + \sqrt{2\beta+1}\,\arctan\frac{1}{\sqrt{2\beta+1}}\sqrt{\frac{(2\beta+1)\tau-1}{1-\tau}},$$

$$V(\tau) = -\frac{U^{\frac{1}{6}}}{q} = \sqrt{2\tau}\,(1-\tau_t)^{\frac{1}{6}}(\tfrac{1}{3})^{\frac{1}{6}}\left\{1 - \frac{3}{5}(1+\tau_t)\left[\frac{(2\beta+1)\tau-1}{1-\tau}\right] + \frac{3}{7}(1+\tau_t+\tau_t^2)\left[\frac{(2\beta+1)\tau-1}{1-\tau}\right]^2 \cdots\right\}^{\frac{1}{2}},$$

$$X(\tau,n) = nU(\tau).$$

These hold uniformly in the one sided neighborhood $\tau_t < \tau < \tau_1$ (τ_1 arb.) of τ_t. A difficulty in the method is that a priori it is not known what linear combination of the asymptotic solutions (55) corresponds to the independent solutions $\tau^{\frac{\lambda}{2}} F_n^{(1)}(\tau)$ and $\tau^{-\frac{\lambda}{2}} F_n^{(2)}(\tau)$, respectively. The precise correspondence was worked out by Seifert [18] and is

$$(56)\quad \tau^{\frac{\gamma}{2}}F_n^{(1)}(\tau) = \frac{\sqrt{\pi}\, e^{n\sigma} n^{\frac{1}{6}} V(\tau) X^{\frac{1}{3}}}{2\sqrt{\tau}\,(1-\tau)^{\beta/2}} \left\{ e^{\frac{i\pi}{6}} H_{\frac{1}{3}}^{(1)}(X)\left[1+\mathcal{O}(\tfrac{1}{n})\right] + e^{-\frac{i\pi}{6}} H_{\frac{1}{3}}^{(2)}(X)\left[1+\mathcal{O}(\tfrac{1}{n})\right] \right\}$$

and

$$\tau^{-\frac{\gamma}{2}}F_n^{(2)}(\tau) = \frac{\sqrt{\pi}\, e^{-n\sigma} n^{\frac{1}{6}} V(\tau) X^{\frac{1}{3}}}{4\sqrt{\tau}(1-\tau)^{\beta/2}\sin n\pi} \left\{ e^{i\pi(n+\frac{1}{6})} H_{\frac{1}{3}}^{(1)}(X)\left[1+\mathcal{O}(\tfrac{1}{n})\right] + e^{-i\pi(n+\frac{1}{6})} H_{\frac{1}{3}}^{(2)}(X)\left[1+\mathcal{O}(\tfrac{1}{n})\right] \right\}$$

where

$$\sigma = -\sqrt{\frac{\gamma+1}{\gamma-1}}\,\operatorname{arctanh}\sqrt{\frac{\gamma-1}{\gamma+1}} + \tfrac{1}{2}\log[2(\gamma-1)] \qquad (= -1.17 \text{ for } \gamma = \tfrac{7}{5}).$$

We aim to find the asymptotic expansion of the particular combination (21) of these two functions, where κ_n is chosen such that

$$\kappa_n = -\left[\frac{d}{d\tau}(\tau^{-\frac{\gamma}{2}}F_n^{(2)}) \Big/ \frac{d}{d\tau}(\tau^{\frac{\gamma}{2}}F_n^{(1)})\right]_{\tau=\tau_t}.$$

Now on differentiating (56) we obtain

$$\frac{d}{d\tau}\left(\tau^{\frac{\gamma}{2}}F_n^{(1)}\right) = \frac{\sqrt{\pi}\, e^{n\sigma} n^{\frac{1}{6}}}{2\sqrt{\pi}\,(1-\tau)^{\beta/2}} \left\{ e^{\frac{i\pi}{6}} \left[V(\tau)\frac{d}{d\tau}[X^{\frac{1}{3}}H_{\frac{1}{3}}^{(1)}(X)] + X^{\frac{1}{3}}H_{\frac{1}{3}}^{(1)}(X)V'(\tau) \right.\right.$$

$$\left. + X^{\frac{1}{3}}H_{\frac{1}{3}}^{(1)}(X)V(\tau)\frac{(1+\beta)\tau-1}{2\tau(1-\tau)}\right][1+\mathcal{O}(\tfrac{1}{n})] + e^{-\frac{i\pi}{6}}\left[V(\tau)\frac{d}{d\tau}[X^{\frac{1}{3}}H_{\frac{1}{3}}^{(2)}(X)]\right.$$

$$\left.\left. + X^{\frac{1}{3}}H_{\frac{1}{3}}^{(2)}(X)V'(\tau) + X^{\frac{1}{3}}H_{\frac{1}{3}}^{(2)}(X)V(\tau)\frac{(1+\beta)\tau-1}{2\tau(1-\tau)}\right][1+\mathcal{O}(\tfrac{1}{n})] \right\}$$

which on using the result

$$\frac{d}{d\tau}[X^{\frac{1}{3}}H_{\frac{1}{3}}^{(j)}(X)] = \frac{d}{dX}[X^{\frac{1}{3}}H_{\frac{1}{3}}^{(j)}(X)]\frac{dX}{d\tau} = e^{\pm\frac{2\pi}{3}i} X^{\frac{1}{3}}H_{\frac{2}{3}}^{(j)}(X)\cdot\frac{n^{\frac{2}{3}}X^{\frac{1}{3}}}{[V(\tau)]^2}$$

$$= \frac{e^{\pm\frac{2\pi}{3}i} n^{\frac{2}{3}}}{[V(\tau)]^2}\left[X^{\frac{2}{3}}H_{\frac{2}{3}}^{(j)}(X)\right] \qquad \begin{pmatrix} j=1 & \text{upper sign} \\ j=2 & \text{lower sign} \end{pmatrix}$$

and the following well-known relations on Bessel functions

$$H_\nu^{(j)}(X) = \pm \frac{i}{\sin \nu\pi}\left[e^{\mp \nu\pi i} J_\nu(X) - J_{-\nu}(X)\right]$$

$$\lim_{\substack{X\to 0 \\ (\tau\to\tau_t)}} X^\nu J_\nu(X) = 0 \qquad \lim_{\substack{X\to 0 \\ (\tau\to\tau_t)}} X^\nu J_{-\nu}(X) = \frac{2^\nu}{\Gamma(1-\nu)}$$

becomes on evaluation at $\tau = \tau_t$

$$\left[\frac{d}{d\tau}(\tau^{\frac{n}{2}} F_n^{(1)})\right]_{\tau=\tau_t} = \frac{\sqrt{\pi}\, e^{n\sigma} n^{\frac{1}{6}}}{2\sqrt{\tau_t}(1-\tau_t)^{\beta/2}} \left\{ e^{\frac{i\pi}{6}} \left[\frac{e^{\frac{2\pi i}{3}} n^{\frac{2}{3}}}{V(\tau_t)} \cdot \frac{-2^{\frac{5}{3}i}}{\sqrt{3}\Gamma(\frac{1}{3})} + \frac{-2^{\frac{4}{3}i}}{\sqrt{3}\Gamma(\frac{2}{3})} \cdot V'(\tau_t) \right.\right.$$

$$\left. + \frac{-2^{\frac{4}{3}i}}{\sqrt{3}\Gamma(\frac{2}{3})} V(\tau_t) \frac{(1+\beta)\tau_t - 1}{2\tau_t(1-\tau_t)} \right] \left[1 + \mathcal{O}(\tfrac{1}{n})\right]$$

$$+ e^{-\frac{i\pi}{6}} \left[\frac{e^{-\frac{2\pi i}{3}} n^{\frac{2}{3}}}{V(\tau_t)} \cdot \frac{+2^{\frac{5}{3}i}}{\sqrt{3}\Gamma(\frac{1}{3})} + \frac{+2^{\frac{4}{3}i}}{\sqrt{3}\Gamma(\frac{2}{3})} \cdot V'(\tau_t) \right.$$

$$\left.\left. + \frac{+2^{\frac{4}{3}i}}{\sqrt{3}\Gamma(\frac{2}{3})} V(\tau_t) \frac{(1+\beta)\tau_t - 1}{2\tau_t(1-\tau_t)} \right] \left[1 + \mathcal{O}(\tfrac{1}{n})\right] \right\}$$

where

$$V(\tau_t) = (\tfrac{8}{3})^{\frac{1}{6}} \tau_t^{\frac{1}{2}} (1-\tau_t)^{\frac{1}{6}}$$

$$V'(\tau_t) = \left[\frac{dV}{d\tau}\right]_{\tau=\tau_t} = \frac{1}{\sqrt{2\tau_t}} (1-\tau_t)^{\frac{1}{6}} (\tfrac{1}{3})^{\frac{1}{6}} \left[1 - \frac{\beta}{5} \frac{2\tau_t(1+\tau_t)}{(1-\tau_t)^2}\right].$$

Similarly

$$\left[\frac{d}{d\tau}(\tau^{-\frac{1}{2}} F_n^{(2)})\right]_{\tau=\tau_t} = \frac{\sqrt{\pi}\, e^{-n\sigma} n^{\frac{1}{6}}}{4\sqrt{\tau_t}(1-\tau_t)^{\beta/2} \sin n\pi} \left\{ e^{i\pi(n+\frac{1}{2})} \left[\frac{e^{\frac{2\pi i}{3}} n^{\frac{2}{3}}}{V(\tau_t)} \cdot \frac{-2^{\frac{5}{3}i}}{\sqrt{3}\Gamma(\frac{1}{3})} + \frac{-2^{\frac{4}{3}i}}{\sqrt{3}\Gamma(\frac{2}{3})} V'(\tau_t) \right.\right.$$

$$\left. + \frac{-2^{\frac{4}{3}i}}{\sqrt{3}\Gamma(\frac{2}{3})} V(\tau_t) \frac{(1+\beta)\tau_t - 1}{2\tau_t(1-\tau_t)} \right] \left[1 + \mathcal{O}(\tfrac{1}{n})\right] + e^{-i\pi(n+\frac{1}{2})} \left[\frac{e^{-\frac{2\pi i}{3}} n^{\frac{2}{3}}}{V(\tau_t)} \cdot \frac{2^{\frac{5}{3}i}}{\sqrt{3}\Gamma(\frac{1}{3})} \right.$$

$$\left.\left. + \frac{+2^{\frac{4}{3}i}}{\sqrt{3}\Gamma(\frac{2}{3})} V'(\tau_t) + \frac{+2^{\frac{4}{3}i}}{\sqrt{3}\Gamma(\frac{2}{3})} V(\tau_t) \frac{(1+\beta)\tau_t - 1}{2\tau_t(1-\tau_t)} \right] \left[1 + \mathcal{O}(\tfrac{1}{n})\right] \right\}.$$

Thus

$$\chi_n = -\frac{e^{-2n\sigma}}{2\sin n\pi}\left\{\frac{e^{i\pi(n+\frac{1}{2})}\left[e^{\frac{2\pi}{3}i}n^{\frac{2}{3}}+\delta\right]\left[1+\mathcal{O}(\frac{1}{n})\right]-e^{-i\pi(n+\frac{1}{2})}\left[e^{-\frac{2\pi}{3}i}n^{\frac{2}{3}}+\delta\right]\left[1+\mathcal{O}(\frac{1}{n})\right]}{e^{i\frac{\pi}{6}}\left[e^{\frac{2\pi}{3}i}n^{\frac{2}{3}}+\delta\right]\left[1+\mathcal{O}(\frac{1}{n})\right]-e^{-i\frac{\pi}{6}}\left[e^{-\frac{2\pi}{3}i}n^{\frac{2}{3}}+\delta\right]\left[1+\mathcal{O}(\frac{1}{n})\right]}\right\}$$

where we have used the abbreviation

$$\delta = \frac{V(\tau_t)\Gamma(\frac{1}{3})}{2^{\frac{1}{3}}\Gamma(\frac{2}{3})}\left[V'(\tau_t)+V(\tau_t)\frac{(1+\beta)\tau_t-1}{2\tau_t(1-\tau_t)}\right].$$

Now forming the sonic limit line combination (53) we have after some lengthy computations

$$P_n(\tau) = -\frac{\sqrt{\pi}\,e^{-n\sigma}n^{\frac{1}{6}}V(\tau)X^{\frac{1}{3}}}{2\sqrt{\tau}(1-\tau)^{\beta/2}}\left\{\frac{(e^{-\frac{2\pi}{3}i}n^{\frac{2}{3}}+\delta)H_{\frac{1}{3}}^{(1)}(X)[1+\mathcal{O}(\frac{1}{n})]+(e^{\frac{2\pi}{3}i}n^{\frac{2}{3}}+\delta)H_{\frac{1}{3}}^{(2)}(X)[1+\mathcal{O}(\frac{1}{n})]}{(n^{\frac{2}{3}}+\beta)[1+\mathcal{O}(\frac{1}{n})]}\right\}$$

and on making use of the asymptotic expansion of the Hankel function*

$$H_{\frac{1}{3}}^{(j)}(X) = \left(\frac{2}{\pi X}\right)^{\frac{1}{2}}e^{\mp Xi\mp\frac{5\pi}{12}i}\left[1+\mathcal{O}(\frac{1}{X})\right]$$

this becomes

$$P_n(\tau) = \frac{\sqrt{2}\,e^{-n\sigma}}{\sqrt{\tau}(1-\tau)^{\beta/2}q(\tau)}\left\{\cos(nU-\frac{13\pi}{12})+\mathcal{O}(\frac{1}{n})\right\}.$$

---

* Watson, G. N. A Treatise on the Theory of Bessel Functions, Cambridge Univ. Press, 1944, 2nd ed., p. 198.

BIBLIOGRAPHY

[1] Chaplygin, S. A. "On gas jets." Sci. Annals Imp. Univ. of Moscow, Phys.-Math. Div., 21, (1904). Available as Brown Univ. translation by M. H. Slud (1944) and NACA TM 1063 (1944).

[2] Craggs, J. W. "The breakdown of the hodograph transformation for irrotational compressible fluid flow in two dimensions." Proc. Camb. Phil. Soc., 44, (1948), 360-379.

[3] . . . . . "The compressible flow corresponding to a line doublet." Quart. Appl. Math., 10., (1952), 88-93.

[4] Davies, H. J. "The two-dimensional irrotational flow of a compressible fluid around a corner." Quart. J. Mech. Appl. Math., 6, (1953), 17-80.

[5] de la Vallée Poussin, Ch.-J. Cours d'Analyse Infinitésimale. Vol. 2, 7th Ed. Louvain: Uystpruyst, 1937 (reprinted New York: Dover, 1946) 357 ff.

[6] Garrick, I. E. and Kaplan, Carl. "On the flow of a compressible fluid by the hodograph method. II - Fundamental set of particular flow solutions of the Chaplygin differential equation." NACA Report 790, (1944).

[7] Geiringer, H. "Grenzlinien der Hodographentransformation." Math. Zeitschr., 63, (1956), 514-524.

[8] Huckel, V. "Tables of hypergeometric functions for use in compressible flow theory." NACA TN 1716, (1948).

[9] Langer, R. E. "On the asymptotic solutions of ordinary differential equations with an application to the Bessel functions of large order." Trans. Amer. Math. Soc., 33, (1931), 23-64.

[10] Lighthill, M. J. "The hodograph method." Chpt. VII in Modern Developments in Fluid Dynamics. High Speed Flow. (Ed. by L. Howarth). Oxford Univ. Press, 1953.

[11] Ludford, G. S. S. and Schot, S. H. "On sonic limit lines in the hodograph method." Math. Zeitschr., 67, (1957), 229-237.

[12] . . . . . (Abstract of [11]) Bullet. Amer. Math. Soc., 63, (1957), 246.

[13] Mises, R. v. Mathematical Theory of Compressible Fluid Flow. (Completed by Hilda Geiringer and G. S. S. Ludford), New York: Academic Press, 1958, 322-325.

[14] O'Brien, V. "Remarks on Chaplygin functions." Johns Hopkins Univ. Appl. Physics Lab. Report CM-871, (1956). See also J. Aeronaut. Sci., (1956), 894-895.

[15] Ringleb, F. "Exakte Lösungen der Differentialgleichungen einer adiabatischen Gasströmung." Zeitschr. angew. Math. Mech., 20, (1940), 185-198, 295-296.

[16] . . . . . "Über die Differentialgleichungen einer adiabatischen Gasströmung und den Strömungsstoss." Deutsche Math., 5, (1940), 377-384.

[17] Sears, W. R. and Kuo, Y. H. "Plane subsonic and transonic potential flows." Section F in General Theory of High Speed Aerodynamics (Ed. by W. R. Sears). Princeton Univ. Press, 1954.

[18] Seifert, H. "Die hypergeometrischen Differentialgleichungen der Gasdynamik." Math. Ann., 120, (1947), 75-126.

[19] Taylor, G. I. "Some cases of flow of compressible fluids." ARC Reports and Memoranda 1382, (1930).

[20] Temple, G. and Yarwood, J. "Compressible flow in a convergent-divergent nozzle." ARC Reports and Memoranda 2077, (1942).

[21] Tollmien, W. "Grenzlinien adiabatischer Potentialströmungen." Zeitschr. angew. Math. Mech., 21, (1941), 140-152, 308.

[22] . . . . . "The direct hodograph method in the theory of the flow of compressible fluids." H. Reissner Anniv. Vol., Contributions to Appl. Mech., Edward Bros., 1949.

[23] Tricomi, F. "Sulle equazioni lineari derivate parziali del secondo ordine, di tipo misto." Memorie Reale Accad. Nazl. Lincei., 14, (ser. 5), (1923), 133-247. Available as Brown Univ. Translation A9-T-26 (1948).

[24] Williams, J. "The two-dimensional irrotational flow of a compressible fluid in the acute region made by two rectilinear walls." Quart. J. Math., 20, (1949), 129-134.